50- 237
50 - 249

3-18-69

ANSWERS TO AEC QUESTIONS

DRESDEN NUCLEAR POWER STATION
UNITS 2 AND 3

AMENDMENT NUMBER 10 FOR UNIT 2
AND
AMENDMENT NUMBER 11 FOR UNIT 3

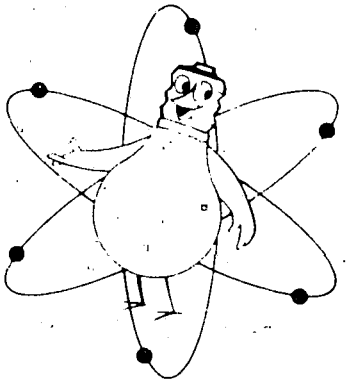

Commonwealth Edison
Company

922

ANSWERS TO AEC QUESTIONS

DRESDEN NUCLEAR POWER STATION
UNITS 2 AND 3

AMENDMENT NUMBER 10 FOR UNIT 2
AND
AMENDMENT NUMBER 11 FOR UNIT 3

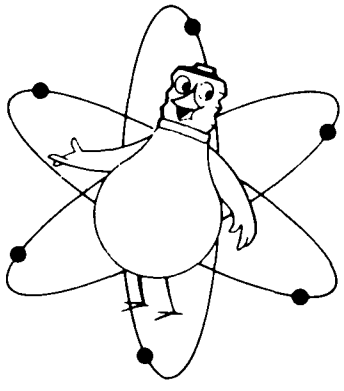

Commonwealth Edison
Company

QUESTION

I. A. 1 Provide detailed descriptions of the analytical methods and models, assumptions, and input and output parameters of the new codes used in the Dresden 2/3 LOCA analysis (LAMB, SCAT, and CHASTE). Describe the calculational sequence using these and the other GE codes (RIP and WAZOO-2), and give the break ranges for which the various codes apply.

ANSWER

A detailed description of the various assumptions and models used will be provided rather than specific codes since the latter are merely ways of executing the actual numerical calculations involved.

There are two basic procedures used in the analysis of loss-of-coolant accidents. The particular procedure used is determined by the size of the break being considered, i.e., "small" breaks or "large" breaks. Small breaks are those for which the blowdown transient is very mild and the associated core heat transfer during the entire flow coastdown is essentially identical to a pump trip transient. All key parameters change relatively slowly with time. The blowdown transient begins to have significant effects for breaks in excess of about 0.5 square feet and are thus classified as "large" breaks. Thus, the transient core flow and heat transfer calculations are performed by a different model which includes the blowdown feedback effects on flow. A general outline of the procedures used, the models involved and the results are outlined in Figure I. A. 1.

Small breaks (less than 0.5 sq. ft.) are analyzed in two steps. The first step is the prediction of the thermal-hydraulic transient which results from a particular break and combination of emergency core cooling systems. The results of this analysis are usually presented in the form of vessel pressure and coolant level as a function of time. Examples of these results can be found in Section 6 of the FSAR, Figures 6.2.6, 6.2.12, 6.2.15, 6.2.28, 6.2.29, and 6.2.30. These results were obtained through the use of the small break thermal-hydraulic analytical model. A complete description of this model (input, output, assumptions) is in Section 6.2.7.1 of the FSAR.

The second step in the analysis of small breaks is the prediction of the peak clad temperatures which result from the accident. The results of the first step, particularly coolant level inside the core shroud, and the core heatup analytical model are used for this purpose. The core heatup analysis gives the peak clad temperature which will be reached

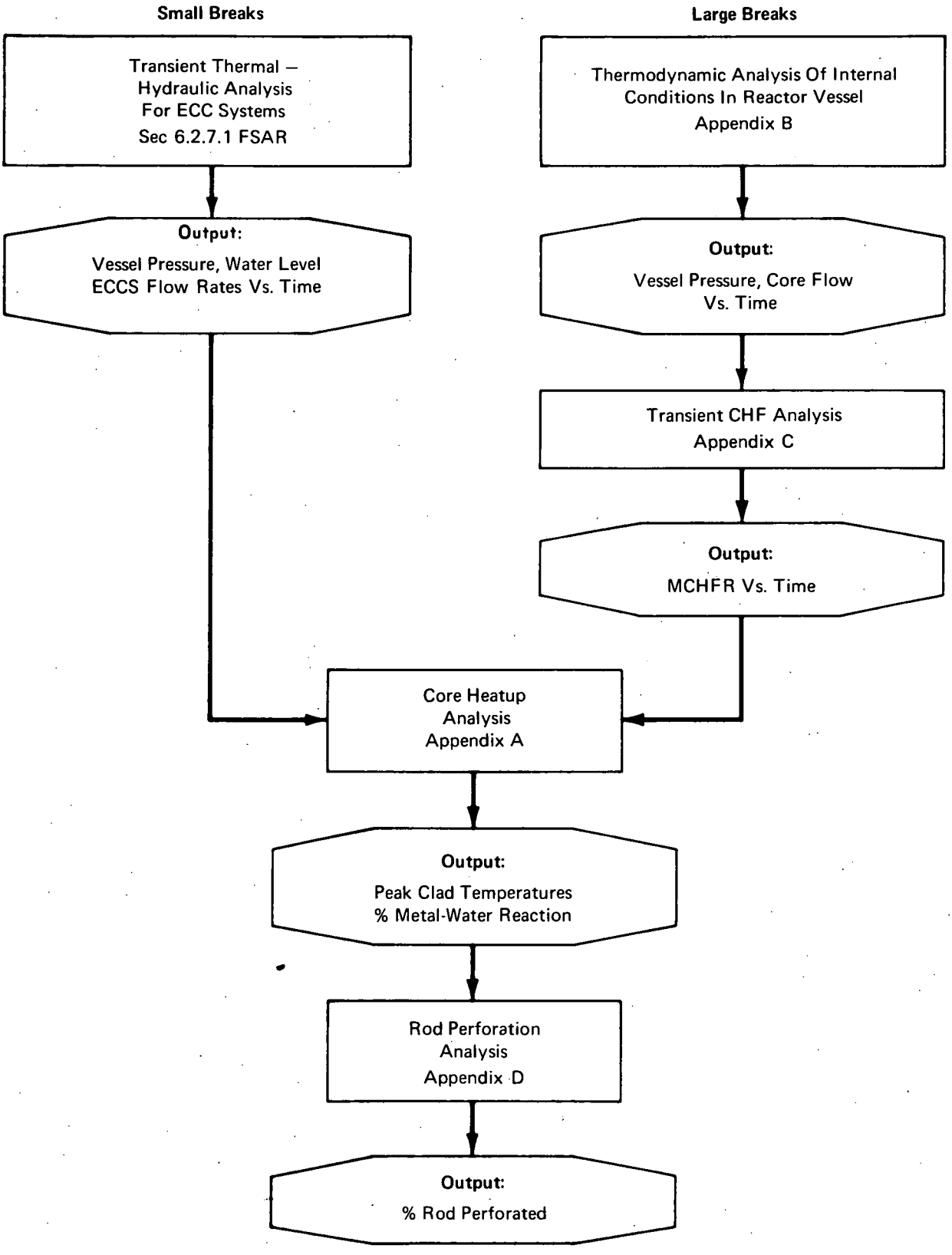

Fig I.A.1 Loss of Coolant Accident Analytical Procedures

in a particular core node (i.e., remained covered with water) and then the amount of time it remained insulated (i.e., uncovered with water). Also, the effect of rated core spray flow on the heatup over the period the core remains uncovered is determined. Details of these calculations can be found in the description of the core heatup analytical model in Appendix A. Obviously then, water level inside the core shroud predicted in the first step from the ECCS thermal-hydraulic analytical model is the means by which the time a particular core node was initially cooled and the time it remained insulated (uncovered) and/or the time at which core spray rated flow was reached is determined. These results applied to the core heatup model give the peak clad temperatures for any combination of core cooling systems and break size (up to about 0.5 sq. ft.). An example of the peak clad temperatures which result from this type of analysis can be seen in Figure 6.2.35 of the FSAR.

Large breaks (greater than 0.5 sq. ft.) are analyzed in three steps. The first step involves the reactor flow analysis during the vessel blowdown. The most important result of this analysis is the predicted core inlet flow during the blowdown. The core inlet flow is important because it is used in step 2 in the critical heat flux transient analysis model to determine if and when MCHFR goes below 1.0. When the MCHFR goes below 1.0, nucleate boiling ceases and the fuel rod clad is assumed to begin to heat up with a convection coefficient equal to zero. (Actually, the MCHFR would have to drop well below one because unity is defined by a line below all the data). The time at which the MCHFR goes below 1.0 can then be put into the core heat up analytical model to determine the clad thermal transient. The clad heatup is terminated either through flooding or the action of the core spray system and the peak clad temperatures which were reached at those times on the temperatures which are illustrated in, for example, Figure 6.2.35 of the FSAR for the maximum recirculation line break.

Detailed descriptions of the large break reactor transient flow model and the critical heat flux analytical model can be found in Appendix B and C, respectively. The core heat up model mentioned above is the same as used in the small break analysis and is described in Appendix A.

A final step is taken in the analysis of loss-of-coolant accidents, for large or small break sizes, after the peak clad temperatures have been determined. That step is the calculation of the percentage of the total number of fuel rods which will perforate. This percentage is conservatively determined through the assumption that the entire core is at the calculated peak clad temperature and the correlation of this temperature with the experimentally determined clad stress limits and predicted internal gas pressures. The reason why the number of rods perforated varies even though all rods are at the same temperature is that perforation is also a function of internal gas pressure and the number of rods at any given pressure varies over a wide range as shown in Appendix D. A complete description of the model used can be found in Appendix D.

APPENDIX A

REACTOR CORE HEATUP MODEL

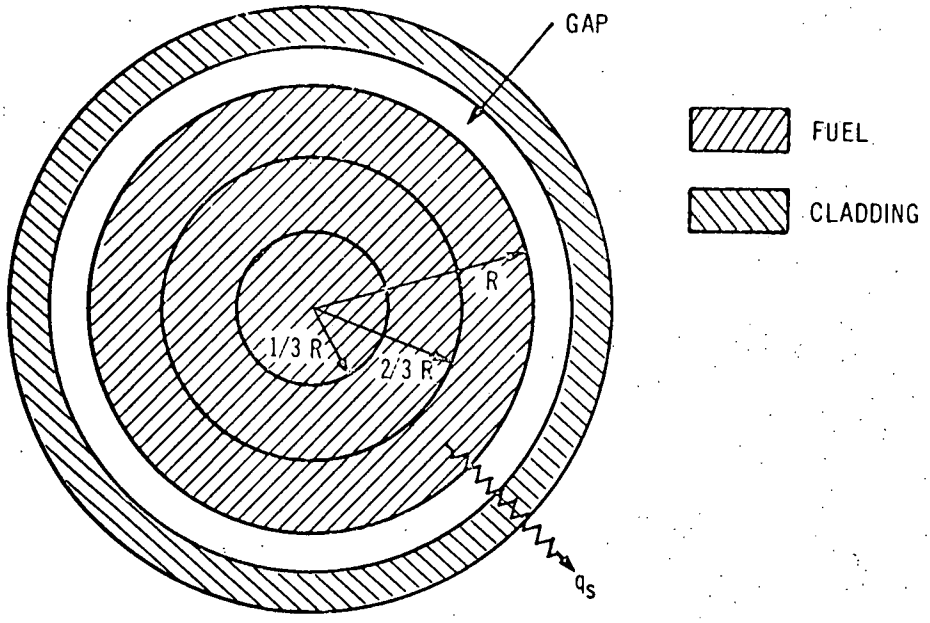

FUEL ROD DETAIL

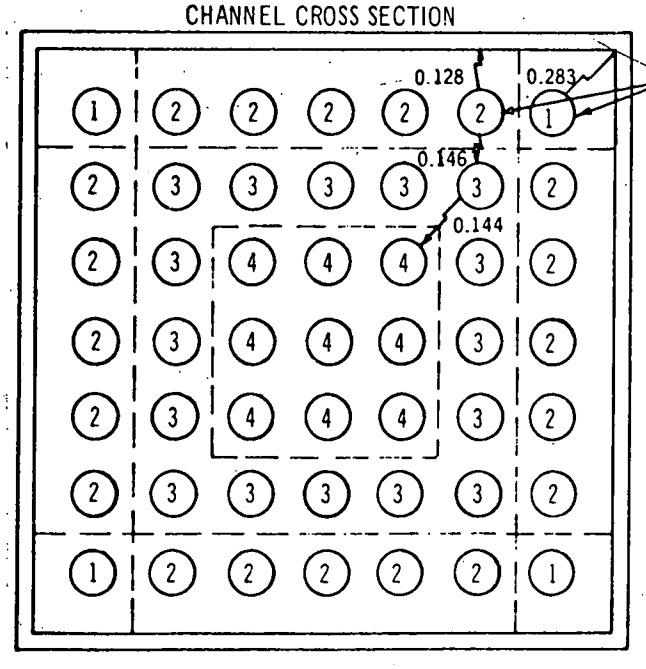

CHANNEL

ROD TYPE	NO OF RODS	ROD POWER FACTOR
1	4	1.3
2	20	1.15
3	16	0.90
4	9	0.70

FUEL BUNDLE DETAIL

FIGURE I.A.2 FUEL ROD AND FUEL BUNDLE DETAILS

REACTOR CORE HEATUP MODEL

Introduction

The analytical method used to calculate the reactor core thermal transient following a loss-of-coolant accident is described in this Appendix and is the same as that described in Amendment #5 of Oyster Creek. The fuel temperature, cladding temperature, channel temperature, and amount of metal-water reaction are calculated as functions of time from the start of the accident. In this analysis the power of decaying fission products, the chemical energy released by metal-water reactions, and the stored heat in the fuel, cladding, and other metal in the core are included as heat sources.

The fuel rods are classified such that those with similar power levels and fuel bundle locations are analyzed as a group. A one-dimensional heat balance is then written for each type of fuel rod. Heat is transferred from the surface of the fuel rods by convection to the water, steam or hydrogen formed in the metal-water reaction. In addition, thermal radiation between fuel rods and from the rods to the channel is accounted for in the overall heat balance.

Theoretical Development

A typical fuel rod consists of uranium dioxide fuel with a Zircaloy cladding. A fuel bundle consists of 49 fuel rods, grouped together to form a square array which is surrounded by a metal channel. Each fuel rod is divided into three radial temperature zones for the numerical calculations as shown in Figure I. A. 2. The cladding, on the other hand, is described by the average cladding temperature, with an outer surface temperature computed from this average temperature. The channel (Figure I. A. 2) is considered to be at a uniform temperature radially. The fuel rods within the channel are divided into four representative zones (Figure I. A. 2) to describe the spatial variation of power generation. The entire reactor core is made up of several hundred fuel bundles and channels. To describe the radial variations of power generation, the core is divided into five radial zones. The fuel rods and channels are divided into five axial regions. Axial conduction between regions is neglected. Each channel is be isolated from the rest of the core so that interactions between adjacent channels is neglected.

Heat Sources

The energy generated by delayed neutrons and decaying fission products is assumed to be uniform within a fuel rod and to have the same radial and axial variation within the core as the steady-state power distribution. The chemical energy released by the metal-water reaction is described by the parabolic rate law given by Baker[1], where the rate of change of the metal

(1) Baker, L. J. and Avins, R. O., "Analyzing the Effects of a Zirconium-Water Reaction," Nucleonics, 23(7), 70-74 (July 1965).

oxide thickness is written as

$$\frac{d\delta}{dt} = \frac{K}{\delta} \exp(-D/T_c) \quad (1)$$

where:

K = Rate coefficient,
T_c = Cladding temperature,
D = Activation coefficient, and
δ = Oxide thickness.

The heat generation rate and hydrogen release rate are proportional to the rate of change of oxide generated. The chemical heat liberated is given as follows:

$$\frac{dQ_c}{dt} = \frac{d\delta}{dt} \Delta H \rho_c A_s, \quad (2)$$

where:

ΔH = Heat of reaction,
ρ_c = Density of metal, and
A_s = Exposed surface area of oxide.

The mass rate of hydrogen generated is

$$\frac{dW_H}{dt} = 2 \frac{d}{dt} \rho_c A_s \frac{N_{H_2}}{N_{METAL}}, \quad (3)$$

where:

W_H = Mass of hydrogen generated and
N = Molecular weight.

The above reaction rate considers that there is an unlimited source of saturated steam available for the reaction. The empirical reaction constants, K and D, are based upon experimental data obtained under conditions where the metal and water are at the same temperature. Therefore, for Equation 1 to be correct the water must be heated to the cladding temperature. The energy required to heat this water is deducted from the total chemical energy added to the system.

Conduction Heat Transfer

The heatup analysis considers only radial conduction of heat from the fuel to the cladding surface. Axial conduction along the fuel rods or to support structures is neglected. Resistance to heat flow through the fuel-cladding gap is taken into account.

Convection Heat Transfer

Heat is transferred from the cladding and channel to the surrounding fluid by thermal radiation and convection. During the blowdown a convection heat transfer coefficient must be calculated. The water level is calculated from the mass inventory in the reactor vessel during the blowdown.* For small breaks, if an axial node is covered with water, the heat transfer coefficient for that node is obtained from the Jens-Lottes correlation for boiling heat transfer:

$$h = \frac{e^{P/900}}{1.829} (Q_S)^{0.75}, \quad (4)$$

where:

P = Reactor pressure, and

Q_S = Surface heat flux.

From experimental work previously performed at General Electric, it has been demonstrated that the full length of a fuel bundle is adequately cooled if the water level is as high as the core midpoint, or even less. To make use of this fact, Equation 4 is used to describe the heat transfer coefficient if the calculated swollen water level is above the node midpoint. When the swollen water level drops below the midpoint of a node, it is treated as being completely uncovered and the heat transfer rate instantaneously diminishes to zero.

For large breaks in the main steam line or recirculation line, the heatup analysis uses the previously calculated results of the predicted MCHFR transient to determine when the transition from nuclear boiling to film boiling occurs. When the MCHFR on the hot rod goes to 1.0, the core is considered insulated until the core spray system reaches rated flow, or until the core is reflooded by the flooding pumps. The other rods of course will not have an MCHFR less than unity until much later in the transient.

Concentrating on the maximum recirculation line break accident, which results in the most severe fuel rod clad thermal transients, a vessel blowdown is typically over in about 30 seconds and the vessel is conservatively assumed to be completely empty at that time. From the time the MCHFR is less than 1, typically 15 seconds after the break, the heat transfer coefficient is set equal to zero. For the case in which a flooding system (LPCI) is assumed to be operating, the heat transfer coefficient remains at zero until a core axial region is recovered, as was the case in the analysis of small breaks. After the axial region is recovered,

* Section 6.2.7.1, FSAR

the Jens-Lottes correlation for nucleate boiling heat transfer applies and the clad is rapidly cooled. As discussed and demonstrated experimentally in Reference 2, the entire core is cooled due to level swell even if it is only half flooded.

For the case in which a core spray system is assumed to be operating, appropriate heat transfer coefficients are applied as soon as the core spray system reaches rated flow. The coefficients used for the core spray mode of cooling are based on the data obtained from extensive core spray tests conducted at General Electric(2).

Radiation

Thermal radiation between fuel rods and the fuel channel box is permitted if they are not covered with water. To simplify calculations, the fuel rods are grouped into four groups. Figure I. A. 2 shows the channel configuration. Group 1 rods exchange radiation with the channel only. Group 2 rods exchange radiation with the channel and Group 3 rods. Group 3 rods exchange radiation with Group 2 rods and Group 4 rods only. Finally, Group 4 rods exchange radiation only with Group 3 rods. Radiation view factors are also calculated for each group of rods. The view factors together with the emissivity and relative areas are converted to radiation coefficients used in the Stephan-Boltzman equation for obtaining the radiant heat transfer. A more detailed description of this conversion is given in Oyster Creek Amendment #5. Figure I. A. 2 illustrates typical radiation coefficients and rod power.

Method of Solution

The fuel, cladding, and channel temperature are calculated at each time step by considering the aforementioned energy consideration. All temperatures are integrated using a simple Euler forward difference method:

$$\phi \quad (t + \Delta t) = \phi(t) + \frac{d\phi(t)}{dt} \Delta t. \qquad 5$$

All physical properties are considered constant with temperature and time. The model utilizes the calculated histories of pressure, water level, and heat transfer coefficients. The sink temperature for all convective heat transfer calculations is determined by the saturation temperature at the given pressure.

(2) Ianni, P. W., "Effectiveness of Core Standby Cooling Systems for General Electric Boiling Water Reactors," General Electric Report APED-5458 (March, 1968)

APPENDIX B

REACTOR TRANSIENT FLOW MODEL

REACTOR TRANSIENT FLOW MODEL

General

The model used to calculate the hydraulic flow transients through the core is fundamentally the same as that described in Vermont Yankee Amendment #3. However, better nodalization, an improved model of the jet pumps, and an improved core model have now been included thus significantly increasing the accuracy and flexibility especially with respect to core flow. This model will be described in the sections that follow.

The hydraulic transients that would follow a large break in the primary system piping are analyzed with a 9 node model that determines the transient pressures and flows in each node during the blowdown of a BWR. Figure I. A. 3 is a block diagram of the system. The nine volume nodes represented in Figure I. A. 4 are:

1. Lower plenum
2. Core
3. Upper plenum
4. Core bypass region
5. Steam separation zone
6. Steam dome
7. Downcomer
8. The recirculation loop associated with the break
9. The recirculation loop not affected by the break

The core and core bypass nodes are each subdivided into 10 common pressure subnodes. This permits accurate calculation of fluid enthalpy within the core and bypass nodes where the fluid enthalpy varies with distance through the core. A single pressure node representation of the other volumes is sufficiently accurate since they closely approximate a homogeneous mixture. Since there can be only very small heat additions from the structural and vessel metal to the fluid during the time of the transient no heat is considered to be added in the other nodes.

The basic differential equations describing each node are the general equations of conservation of mass;

$$\dot{M} = W_{in} - W_{out} + \int \frac{d\dot{V}}{v} \qquad (1)$$

conservation of volume;

$$\dot{V} = \dot{M}v + \dot{v}M \qquad (2)$$

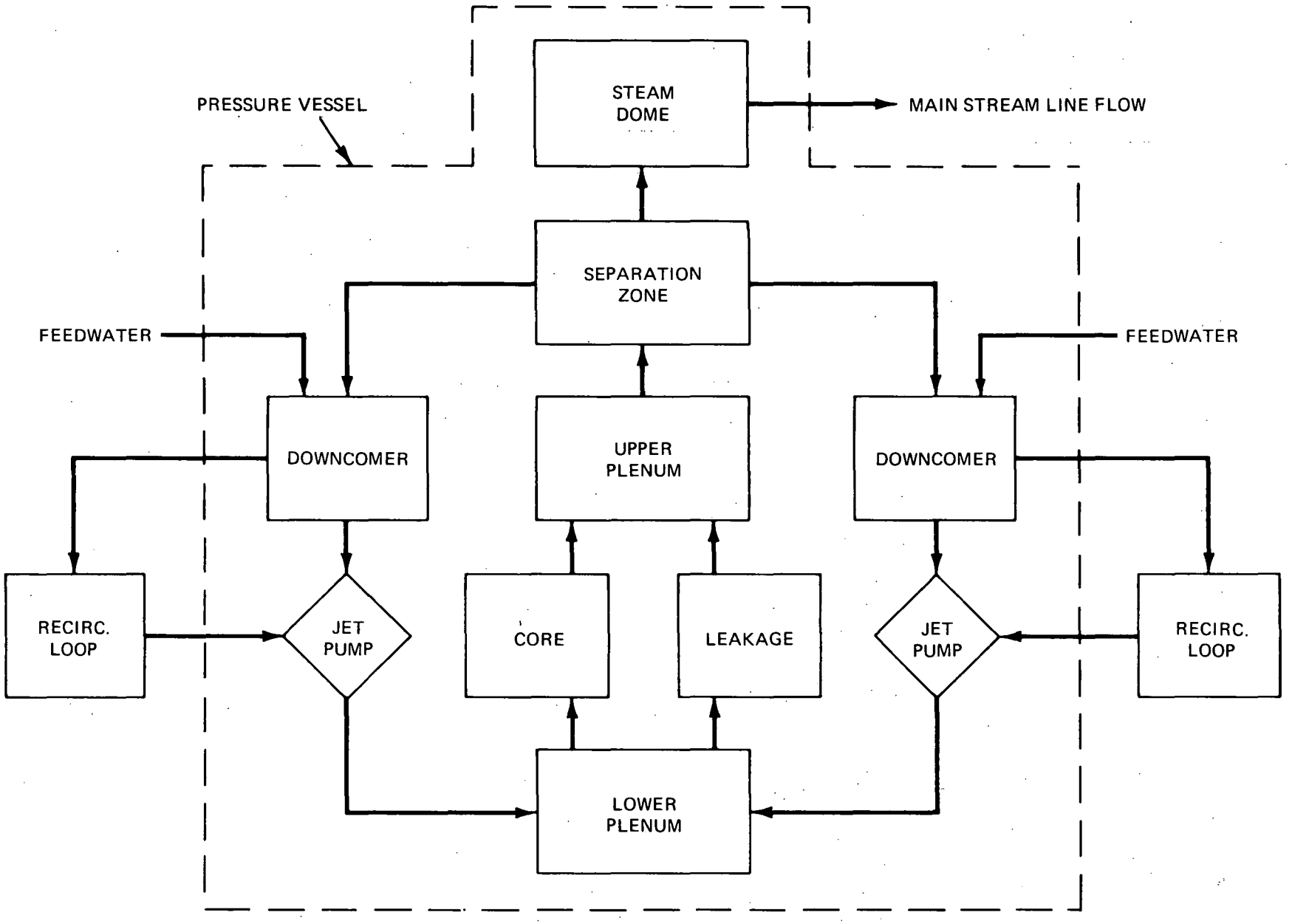

Fig I. A. 3 Large Break Thermo-Hydraulic Transient Model

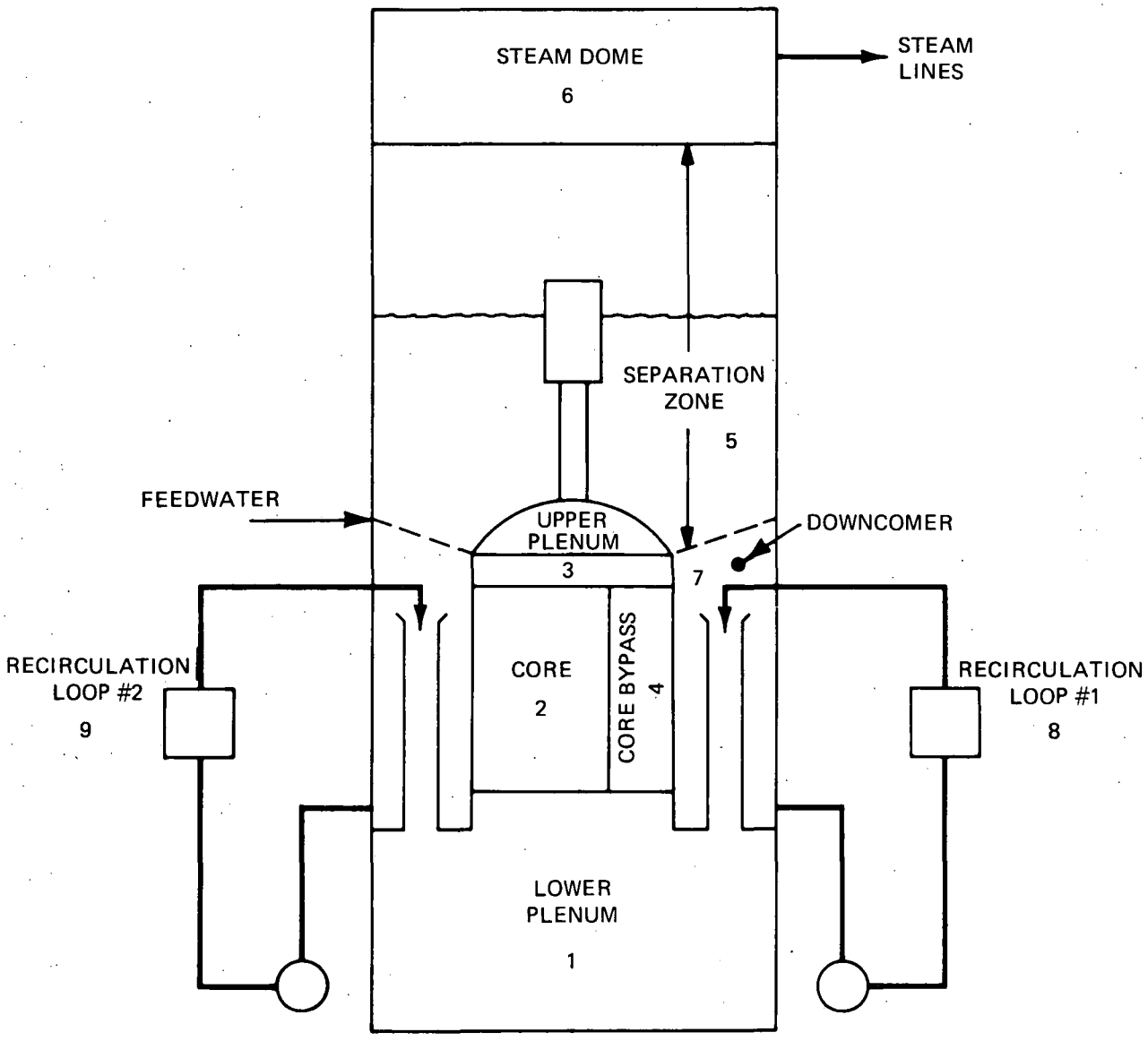

Fig I. A. 4 Schematic Diagram Of BWR Pressure Vessel Nodalization

and conservation of energy.

$$E_{in} - E_{out} + Q = \dot{M}h + \dot{h}M - \alpha V \dot{P} \quad (3)$$

Internodal flow is calculated with the general fluid acceleration equations.

$$\dot{W} = g\frac{A}{L} \cdot \left[\begin{array}{l}\text{nodal pressure difference + Pump head +} \\ \text{Elevation head - irreversible losses}\end{array}\right] \quad (4)$$

Each node is assumed to be of constant volume. The fluid contained in the nodes consists of either liquid and vapor in saturated equilibrium or liquid only in a subcooled state as determined by the energy and mass balances at any given time. Except for the separation region node, the no-slip fluid state equations are used. The model used in the separation node is described below.

External Flows

There are several ways in which fluid may be added to or removed from the pressure vessel during the transient.

a. Feedwater inlet flow can be specified as a function of time in tabular form. If a break in the feedwater line is being examined, fluid is removed from the vessel at the critical flow rate through the break.

b. Steam flow through unbroken steam lines can be specified as a function of time or steam dome pressure in tabular form or as limiting critical flow through closing isolation valves.

c. Steam flow from a break in a steam line is determined by critical flow through the break. This may be limited by steam line restrictions such as flow limiters or closing isolation valves.

d. Fluid may be removed from the system at the critical flow rate through a break in one of the recirculation loops. The break area may vary in size from a small leak to a large complete double ended break. The flow from the large breaks will be limited by critical flow through the drive pump and reverse critical flow through the jet pump drive nozzle.

The break area and any associated friction for each of the above breaks can be specified as a function of time in tabular form. However, the Moody[1] critical flow model assuming no friction is used to calculate all critical flow rates and a sudden break is postulated.

Recirculation System

The flows between nodes are analyzed using the fluid acceleration equation (Equation 4). The flow resistances and elevation effects are calculated from the input quantities of nodal initial pressures, flows, and elevations. During the subsequent transient, the effects of the varying specific volumes are accounted for. The Martinelli-Nelson two-phase friction multipliers are used to calculate frictional pressure drops. The necessary inertial characteristics of each flow path are calculated from the flow path geometry.

The jet pump model is described in detail in the answer to question I. A. 2. The drive pumps are defined by a three dimensional input table of head versus flow for each drive pump. The third dimension included is fluid quality at the drive pump suction. This feature allows the effect of cavitation upon drive pump performance to be included. However, for the recirculation line break the jet pump suction uncovers before saturation occurs at the drive pump inlet. When the jet pump suction uncovers, the flow is assumed to drop to zero.

The effects upon the system of a loss of power to the drive pump motor is also represented. This is based on the initial value of pump/motor inertia and rotational velocity. Pump rundown evaluation is then based upon an analysis which includes the pump speed decay, loop losses and fluid momentum.

Core Power

The heat passing from the fuel to the coolant flowing through the core is calculated from the initial value of heat flux which is decayed as a function of time based on the power decay due to voiding and the fuel time constant. The fraction of the total core heat which reaches the core bypass flow is held constant at the initial value. The assumed axial distribution of the heat passing to both the core and core bypass flow is assumed to remain at its initial value throughout the transient.

Separation Zone Node

The fluid in the separation region is assumed to be heterogeneous in enthalpy and quality and is assumed to have no spatial variations in pressure. Steam carryunder from the

(1) Moody, F. J., "Maximum Flow Rate of a Single Component Two-phase Mixture," Journal of Heat Transfer, ASME Series C, Volume 87, February, 1965.

separators is included as a function of the two-phase mixture level. The quality of this mixture is assumed to be distributed linearly in the vertical direction. When and if, the fluid in the downcomer becomes saturated, the separation region and the downcomer nodes are combined. Variations in water surface level are calculated by a continuous integration of the mixture volume. Free separation of steam from the surface is calculated based on the surface quality and a 1 fps steam bubble relative rise velocity. It should be noted that the level rise model used here is only for finding the carryunder as a function of level to account for proper mass and energy balances and depressurization. The level rise used in the core to determine core cooling is described in Appendix A. The basic phenomena are discussed in Reference (2).

Break Area

For a recirculation line break, the entire area of both ends of the guillotine rupture is defined as the break area. On one side the minimum area of choked flow is assumed to be the cross-sectional area of the main recirculation line. On the other side the flow will be limited by the combined area of 10 jet pump nozzles.

Determination of Output

The coupled equations governing each of the phenomena discussed above for each node are solved in a step wise manner by a computer. Thus, the interdependency of each node, with respect to all variables such as flow rates, pump performance, and pressures are properly evaluated as a function of time. The core flow from this model is then used as an input in the transient critical heat flux model to determine when the MCHFR drops below unity.

(2) Moody, F. J., "Liquid/Vapor Action in a Vessel During Blowdown," ASME Winter Annual Meeting, Paper No. 68-WA/NE-2.

NOMENCLATURE

$\dot{M}$	=	rate of mass change
W	=	mass flow rate
V	=	volume of node
v	=	specific volume in node
E	=	energy in node
h	=	enthalphy
Q	=	energy transferred to node
α	=	void fraction
g	=	gravitational constant
A	=	equivalent area between nodes
L	=	equivalent length between nodes

APPENDIX C

CRITICAL HEAT FLUX TRANSIENT MODEL

TRANSIENT MINIMUM CRITICAL HEAT FLUX MODEL

The analysis calculates the minimum critical heat flux ratio which will occur in a fuel bundle under varying conditions of core inlet flow, enthalpy, pressure and power generation.

This purpose is accomplished by comparing the locally calculated heat flux to the critical heat flux for that region. The local heat flux (among the other parameters) is determined through the simultaneous solution of coupled, time dependent partial differential equations satisfying mass and energy conservation, considering the local power generation and rod time constants, heat transfer coefficients, and the effects of the energy addition on the fluid.

The ratio then of the critical heat flux, which is empirically determined as a function of the predicted fluid mass flow rate and quality (see Figure 6.2.24 of the FSAR) and the calculated local heat flux defines the critical heat flux ratios, with MCHFR being the minimum value which occurs axially at a given point in time.

The major inputs to the model are fuel channel inlet mass flow rate, enthalpy, pressure and bundle power generation rate. The major outputs are MCHFR, the axial values of critical heat flux ratio and average heat flux, mass flow rate, fluid temperature, quality and void fraction, and fuel temperatures.

For calculational purposes, a single fuel rod is considered which has an average power generation rate for the bundle being analyzed and constant axial and radial power shapes. MCHFR, however, is determined for the hottest rod in the bundle. This is done by multiplying the average local heat flux by the hot rod's peaking factor (i.e., multiplying by the ratio of its power operation rate over the average rods power generation rate). Only radial heat transfer in the fuel rod is considered in the calculations, axial and circumferential heat transfer being negligible. The thermal properties of the fuel and clad are functions of temperature and are, therefore, continuously calculated and modified accordingly throughout the transient.

TRANSIENT MINIMUM CRITICAL HEAT FLUX MODEL

The analysis calculates the minimum critical heat flux ratio which will occur in a fuel bundle under varying conditions of core inlet flow, enthalpy, pressure and power generation.

This purpose is accomplished by comparing the locally calculated heat flux to the critical heat flux for that region. The local heat flux (among the other parameters) is determined through the simultaneous solution of coupled, time dependent partial differential equations satisfying mass and energy conservation, considering the local power generation and rod time constants, heat transfer coefficients, and the effects of the energy addition on the fluid.

The ratio then of the critical heat flux, which is empirically determined as a function of the predicted fluid mass flow rate and quality (see Figure 6.2.24 of the FSAR) and the calculated local heat flux defines the critical heat flux ratios, with MCHFR being the minimum value which occurs axially at a given point in time.

The major inputs to the model are fuel channel inlet mass flow rate, enthalpy, pressure and bundle power generation rate. The major outputs are MCHFR, the axial values of critical heat flux ratio and average heat flux, mass flow rate, fluid temperature, quality and void fraction, and fuel temperatures.

For calculational purposes, a single fuel rod is considered which has an average power generation rate for the bundle being analyzed and constant axial and radial power shapes. MCHFR, however, is determined for the hottest rod in the bundle. This is done by multiplying the average local heat flux by the hot rod's peaking factor (i.e., multiplying by the ratio of its power operation rate over the average rods power generation rate). Only radial heat transfer in the fuel rod is considered in the calculations, axial and circumferential heat transfer being negligible. The thermal properties of the fuel and clad are functions of temperature and are, therefore, continuously calculated and modified accordingly throughout the transient.

APPENDIX D

ROD PERFORATION MODEL

ROD PERFORATION MODEL

Included as part of the ECCS performance analyses is the prediction of the number of fuel rods which would perforate expressed as a percentage of the total number of fuel rods in the core. This analysis is the same as that described in Oyster Creek Amendment # 10, Docket 50-219. The perforations are a function of the predicted peak clad temperatures and are based on experimentally determined internal gas pressure distribution and perforation stress data.[1] A rod is assumed to be perforated when the internal pressure is high enough to cause a hoop stress equal to the ultimate strength of the clad at the clad temperature. The ultimate strength of Zircaloy has been experimentally determined. A plot of perforation internal gas pressure, stress at perforation, and the ultimate strength of Zircaloy at various temperatures is presented in Figure I. A. 5. The data is used with the heatup analysis discussed in Appendix A to determine percent rod perforation.

The calculations made to determine rod perforations are supported by test results. The evaluation of the number of perforations occurring for a loss of coolant accident analysis considers the distribution of internal gas pressure in the various rods, the distribution of the rod temperatures, and the actual stress to failure as shown in Figure I. A. 5.

The calculated internal gas pressure distribution within the core is shown in Figure I. A. 6. This distribution is obtained by integrating the expected fission gas release rate for normal operation to the end of an equilibrium cycle when the accumulated fission products are maximum. In addition, the partial pressure of volatile materials and initial gas pressure is included.

The predicted perforations are conservatively high for several reasons. First, the entire core is assumed to be at the predicted peak clad temperature, whereas, only one area of one rod in the entire core would be at the peak temperature. The internal gas pressure distribution, which was calculated using the TVA core as a model, is considered applicable to lower power density cores (i. e., cores with a peak power density of 17. 5 kw/ft compared to the TVA value of 18. 5 kw/ft) in a conservative direction because the higher power density results in a higher fission gas release rate and higher internal gas pressures. Other conservatisms

---

(1) Oyster Creek, Amendment 10, Appendix B.

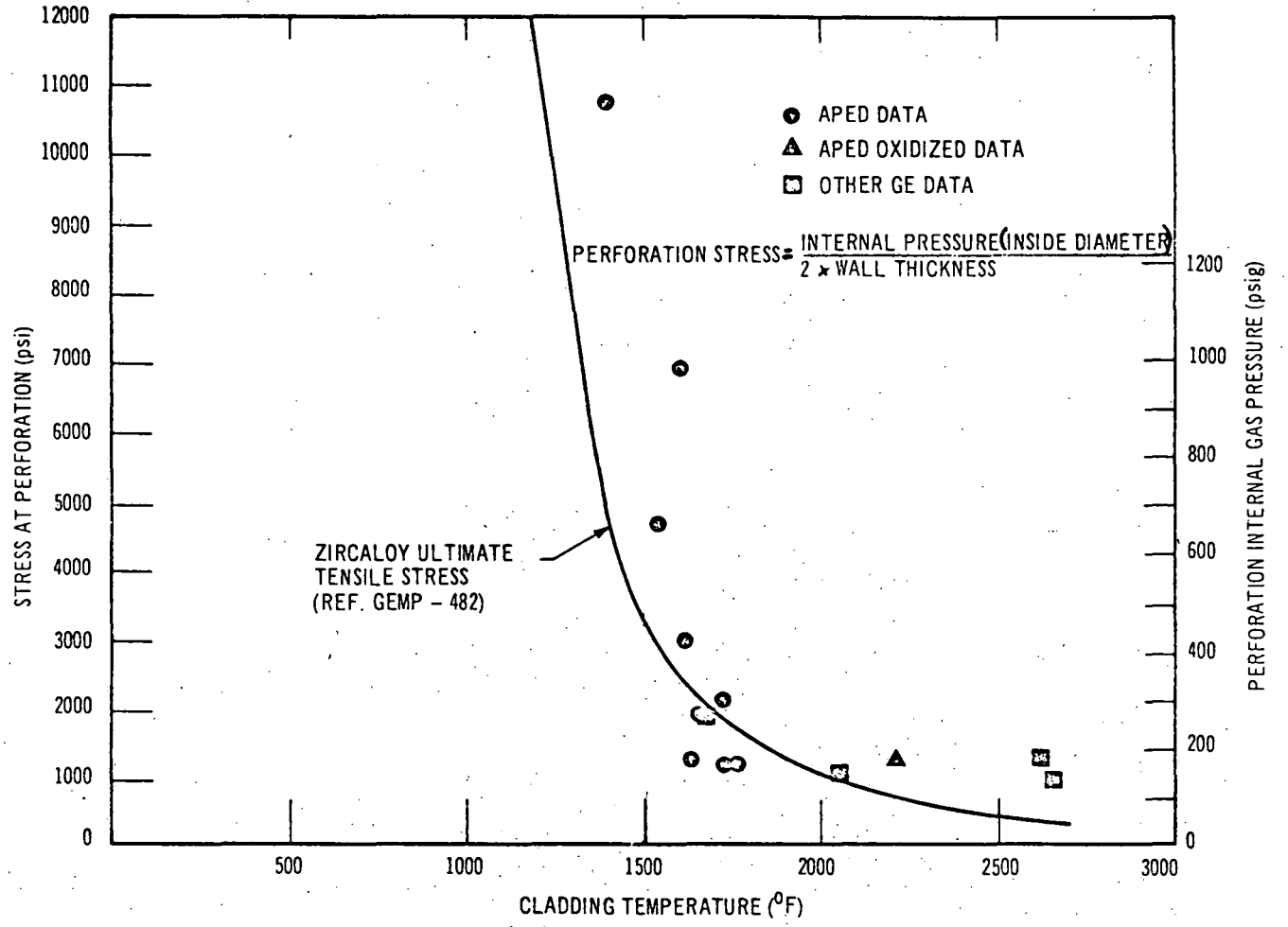

FIGURE I.A.5 PERFORATION STRESS AND PERFORATION INTERNAL GAS PRESSURE AS A FUNCTION OF CLADDING TEMPERATURE

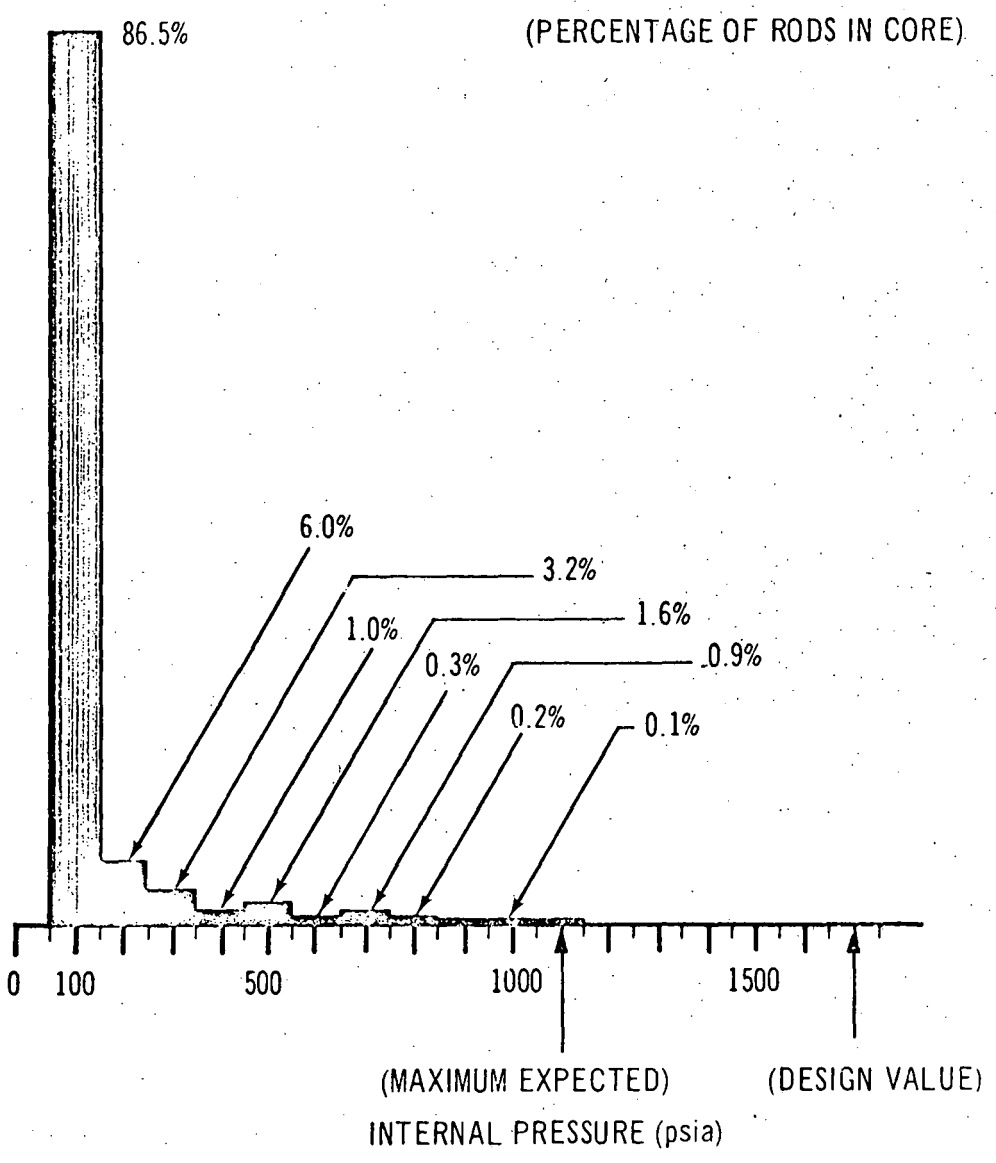

FIGURE I.A.6 DISTRIBUTION OF INTERNAL PRESSURE WITHIN RODS

in the model include (a) the assumption that the peak axial peaking factor existed over 80 percent of the rod length to obtain the fission gas release, and (b) the assumption that high exposure rods would remain at the peak power positions throughout the life of the fuel. These assumptions assured a conservatively high release rate and internal gas pressure. Finally, the assumption that all rods are at the peak temperature ensures a conservative number of perforations since in reality in addition to the various rods being subjected to different pressures, a temperature distribution also exists which if taken into account will reduce the number of perforations.

The perforation stress data were based on unirradiated clad material. But data obtained at General Electric[2] have shown that irradiation effects (higher strength, lower ductility) are annealed out above about 800 ° F. Therefore, the data are assumed to be applicable for irradiated as well as unirradiated clad material.

(2) "Recommended Property and Reaction Kinetics Data for Use in Evaluating a Light-Water-Cooled Reaction Loss-of-Coolant Incident Involving Zircaloy-4 or 304 55-Clad UO_2," GEMP-482 (NMPO).

QUESTION

I.A.2 What are the bases for the conclusions that during blowdown: (a) all of the coastdown flow from the unaffected recirculation loop goes through the core, and (b) there is a 50%-50% flow split between the core and the jet pumps during the period of flashing in the lower plenum.

ANSWER

(a) All the coastdown flow from the unaffected loop goes through the core because, as will be shown below, no flow will bypass the core up through the jet pumps of the broken loop. Flow reversal will not occur in the broken side jet pumps. Thus, all the flow injected into the bottom plenum must go through the core. The conclusion that during the early stages of the blowdown the coastdown flow from the unaffected recirculation loop goes through the core is based upon the predictions of a computerized model of the entire reactor recirculation system. The model includes a momentum exchange simulation of the jet pumps that can analyze their performance under all operating conditions.

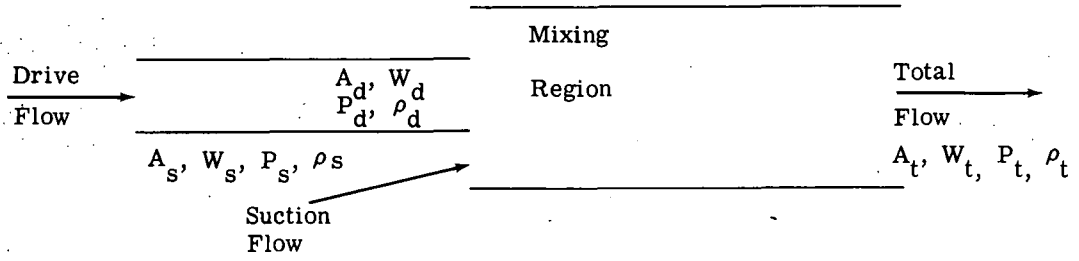

A - Area
W - Mass Flow Rate
P - Pressure
ρ - Density

The above sketch represents the model used in the analysis of transient jet pump performance. Momentum exchange between the drive and suction flows is assumed to occur in a mixing region in the jet pump throat. The suction and drive flows enter

the mixing region with different velocities but at a common static pressure ($P_{di} = P_s$); at the exit of the mixing length a homogeneous velocity is established and momentum exchange between the two flows results in an increased static pressure.

The conservation of momentum law states that the rate of change of momentum of a body is equal to the summation of all the forces acting on that body*, i.e.,

$$\sum \text{Forces} = \frac{d}{dt}(MV)$$

$$= \frac{\partial}{\partial t}(w\,V) + \int V dw_{out} - \int V dw_{in} \qquad (1)$$

For this application, the above equation can be solved in terms of the change of fluid momentum from inlet to exit of the mixing region.

For the linear loss-less mixing region, the only forces acting on the fluid are the static pressures at the inlet and outlet sections. Elevation terms have been neglected; this implies that the momentum exchange occurs a short distance . Hence,

$$\sum F dt = (P_s A_s + P_d A_d - P_t A_t)\, dt \qquad (2)$$

Combination of equations yields

$$P_t = \left(P_s A_s + P_d A_d + \frac{W_d^2}{\rho_d A_d g} + \frac{W_s^2}{\rho_s A_s g} - \frac{W_t^2}{\rho_t A_t g}\right) \cdot \frac{1}{A_t} \qquad (3)$$

Thus the total pressure rise between the downcomer region of the reactor and the entrance to the diffuser section of the jet jumps is given by

$$P_t + \frac{W_t^2}{2g\,\rho_t A_t^2} - \left[P_s + \frac{W_s^2}{2g\,\rho_s A_s^2} + C W_s^2\right]$$

where c is the friction coefficient for flow in the jet pump suction.

This model is used to analyze the transient performance of the jet pumps under all possible modes of operation.

Following the failure of a main recirculation line, the flow in the 10 drive nozzles in the broken loop will very rapidly reverse and critical flow will become established

---

* Shapiro, "Compressible Fluid Flow", Vol. I, pg. 17.

at the nozzles. The fluid leaving the vessel annulus through the jet nozzle at high velocity imparts significant forward momentum to the fluid in the jet pump. When analyzing this mode of operation with the above model, it is calculated that during the early part of the transient there would actually be a positive total flow induced through the jet pumps of the broken loop. However, this positive forward flow is neglected in our analyses and it is merely assumed that no reverse flow occurs through the jet pumps of the broken loop while the suction inlet of the jet pumps is covered with water. That sufficient induced positive pressure to prevent flow reversal in the jet pumps of the broken line will indeed occur can be demonstrated by a numerical example. Substituting the physical constants and solving equation 3 reveals that a positive jet pump shutoff head (i.e., pressure with zero diffuser flow) in excess of about 20 psi. The pressure difference between the lower plenum and the downcomer drops to less than 10 psi during blowdown. (See answer to Question I.A.3). Since the induced equivalent shut off head of the jet pump is well in excess of this amount, it is clear that plenum flow will be prevented from bypassing the core through the broken loop jet pumps. Thus all the flow from the unbroken loop must go through the core until such time that the top of the jet pump uncovers.

(b) When the mixture in the downcomer region of the reactor is completely discharged through the broken recirculation line, the depressurization rate in the vessel will increase markedly since steam will be leaving through the break rather than liquid. This will produce vigorous flashing of the lower vessel plenum inventory, resulting in high flow rates into the core and backwards through both sets of jet pump diffusers. The split of the flow leaving the lower plenum depends upon the resistances of three flow paths, i.e., through the unbroken side jet pumps, through the core, and through the broken side jet pumps. The reverse flow resistances of the two sets of jet pumps are calculated using the following models.

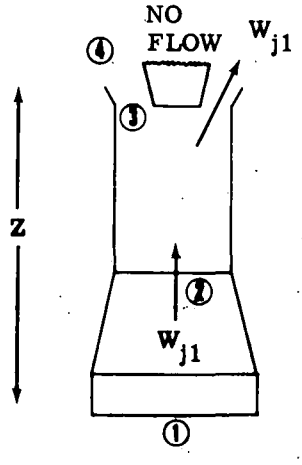

a) Unbroken Recirculation Loop

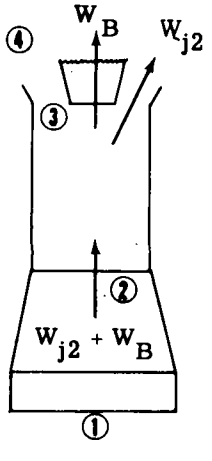

b) Broken Recirculation Loop

Since it is conservative for the reverse flow in the jet pumps to have a low resistance, the minimum expected loss coefficients are used.

If the area of the jet pump throat is A_T and the specific volume of the flow leaving the lower plenum is v ; the total pressure loss between 1 and 4 is

$$\frac{K_{1-4} \cdot W_{j1}^2 \cdot v}{2g\, A_t^2} + \frac{Z}{v}$$

for case a), and

$$\frac{K_{1-3} \cdot (W_{j2} + W_B)^2 \cdot v}{2g\, A_t^2} + \frac{K_{3-4} \cdot W_{j2}^2 \cdot v}{2g\, A_t^2} + \frac{Z}{v}$$

for case b).

W_B is calculated by assuming critical flow at the minimum nozzle area and applying the Moody blowdown model*.

For flow through the core, the total pressure loss between core inlet and outlet is given by an expression of the form

$$K_c \cdot W_c^2 + \frac{Z_c}{v}$$

where W_c is the total core flow, Z_c is the vertical length of the flow path, K_c is a loss coefficient and v is the flow specific volume.

For flow into and through the steam separators, the total pressure drop is given by:

$$K_s \cdot W_c^2 \cdot v. + \frac{Z_s}{v}$$

where Z_s is the distance between the core outlet and the separator outlet.

The flow split between the three available flow paths is calculated by equating the total pressure losses in each of the paths and solving the three equations. For example, when the lower plenum begins to flash the total flow is about 50,000 lb/sec.

---

* Moody, F. J., "Maximum Two Phase Vessel Blowdown from Pipes" ASME Paper No. 65-WA/HT-1.

Substituting 0.36 ft^2 for the area of each jet pump throat, the elevation terms, the specific volume, and loss factors of $.75 \times 10^{-6}$ $\frac{Sec^2}{in^2 ft^3}$ and $.15 \times 10^{-6}$ $\frac{Sec^2}{in^2 ft^3}$ the separator loss coefficients respectively, it is found upon solving the above equations that 28,000 lb/sec will go through the core and 22,000 lb/sec will go backwards through the 20 jet pumps.

The peak clad temperatures are not extremely sensitive to reduced flow split later in the transient. A reduced flow split would result in a shorter period of high heat transfer rates and an earlier start of core heatup. If the split were about 10 percentage points less, the core would begin to blanket 1 second sooner which would result in only a 50°F increase in peak temperature.

QUESTION

I. A. 3 Provide the basis for applying the results of GE's dryout cooling tests to non-jet pump plants and not to jet pump plants. Support the implied conclusion that core flow reversals do not occur during blowdown for Dresden 2/3.

ANSWER

Dryout cooling is a term used to summarize the observation that, when flow is instantly stagnated from its rated value, a fuel rod will be highly cooled by nucleate boiling for only a few seconds followed by a rapidly degenerating heat transfer. These heat transfer test results were obtained in 1965 for non jet pump plants and reported in detail in Topical Report APED-5458. These tests were intended to simulate as closely as possible the conditions to be expected in the non-jet pump BWR, which experiences very rapid core flow stoppage following a design recirculation line break. The test rig used to evaluate heat transfer during vessel blowdown caused by a postulated loss of coolant accident was based on the design configuration for the non-jet pump BWR. For the postulated recirculation line break the depressurization of the lower core plenum would cause essentailly an instantaneous core flow stoppage. Furthermore, the response time in the unaffected recirculation lines is so slow that the recirculation pumps could not provide sufficient flow into core inlet plenum to make up for the loss through the break. In the test rig the system pump was isolated thereby completely eliminating additional flow to the core inlet plenum. Therefore, the measured dryout heat transfer coefficients would apply only to the non-jet pump plant since they simulated sudden flow stoppage.

Basically flow reversals or flow stagnations do not occur in a jet pump plant because blowdown cannot occur directly out of the bottom plenum. Only when the jet pumps are uncovered or when the recirculation pumps cavitate, thus reducing the driving flow, can flow leave the bottom plenum via the jet pumps without going through the core. (See Answer I. A. 2) Calculations using the reactor transient flow model show that during blowdown the pressure in the bottom plenum remains higher than in the other modes. Thus flow must go through the core during the time of interest. As discussed in the answer to question I. A. 2 backward flow up through the jet pumps on the broken side of the recirculation system does not occur until later in the transient when the top of the jet pumps are uncovered.

The recirculation pump in the unaffacted line will continue to provide flow into the core inlet plenum thereby insuring positive core flow. Flow will be continuously injected into the core inlet plenum until the water level in the downcomer section drops sufficiently low to uncover the jet pump nozzles. By the time this occurs, rapid depressurization from steam blowdown causes the bottom plenum to flash forcing flow up the core and up through the jet pumps. The heat added to the core is not sufficient to cause flow reversal since the core heat flux will have dropped significantly at this time in the transient.

Typically for example, the pressures in the key vessel volumes vary while the flow is coasting down as shown in the table below.

TOTAL PRESSURES DURING
A RECIRCULATION LINE BREAK (PSIA)

Vessel Region	TIME - SECONDS 0	4	7
Lower Plenum	1045	997	976
Core	1030	993	974
Upper Plenum	1022	990	973
Downcomer	1015	987	973
Steam Dome	1010	985	973

It will be noted that the pressure is always higher below the core. Also the absolute pressure levels are well above the pressure at which the recirculation pumps will cavitate and thus flow will continue to be injected into the bottom plenum. Therefore, for a jet pump plant the flow through the core continues long enough to avoid violating the MCHFR while the heat flux is still high. For this reason the dryout tests are not applicable. As explained in the answer to Question I. A. 5, later in the transient the MCHFR does drop below unity and the hot rod is assumed to be insulated. The dryout data is not used for the jet pump plant analysis.

QUESTION

I.A.4 Describe the method used to calculate the radial core flow distribution during blowdown. Describe how this calculation demonstrates that all fuel bundles receive adequate flow, and discuss the basis for applying your chosen heat transfer correlation to the complete range of calculated flow conditions.

ANSWER

For a design recirculation or steam line break, the core flow and MCHFR are calculated as a function of time for the first 10-20 seconds, while the flow through the core is coasting down. Since for the maximum steam line break there is no temperature rise, (the fuel clad temperature decreases monotonically from time zero,) this discussion will be directed primarily at the recirculation line break, which results in peak temperature in the neighborhood of 2000 F.

By use of a multi-channel model the core is orificed for normal operation to direct larger amounts of flow to the higher power bundles. Also, it is ensured by design criteria that the channel hydraulic characteristics are "stiff", i.e., that they have sufficient single phase pressure drop so as not to change the channel flow significantly if perturbations were to occur inside individual channels. For the recirculation line break, the reactor transient flow model shows that the flow through the core diminishes to about 1/3 of the rated value during the transient time of interest. Over such a flow range the overall core will act as a unit with respect to flow since each channel is exposed to the same pressure differential between the upper and lower plenum. Furthermore, the core heat flux is decreasing at about the same rate as the flow during this time so that the overall core hydraulic characteristics with respect to exit voids do not change a great deal. Therefore, flow re-apportionment due to pressure differences across the core should not occur during the transient.

Changes in void fraction across the core could cause re-apportionment but flow in any given channel is a weak function of exit voids. Furthermore, the heat flux over the entire core will decrease at the same rate due to the overall void increase or scrammed control rods. Thus, large relative void changes are precluded.

The question of flow reapportionment during the flow coastdown following a loss of coolant transient has also been analyzed quantitatively using the transient CHF analysis model described in Appendix C. This analysis was used to calculate the pressure drop across different fuel channels as a function of time, assuming no redistribution of flow from the initial steady-state distribution prior to the loss of coolant accident. The transient pressure drop

across these fuel bundles was then compared. The variation in pressure drop from bundle to bundle at any time was always less than 10% for the two extremes. Physically in the actual case the pressure drop across each bundle must be the same as all other bundles at all times because they are all exposed to the same plenums. Therefore, there will be a small variation in the flow distribution with time between channels. However, the flow through any bundle will be proportional to the square root of the pressure drop; hence, the flow maldistribution between bundles will always be less than 5%. This is an insignificant variation for the loss of coolant transient.

For the reasons above, the assumption that the flow distribution through the core during a loss of coolant transient is unchanged from the steady-state distribution is justifiable.

The basis for applying the chosen heat transfer correlation to the complete range of calculated flow conditions is discussed in the answer to Question I.A.5.

QUESTION

I.A.5 Please provide justification for the application of the steady state Hench-Levy CHF correlation to a system undergoing a rapid pressure transient. Indicate the break range for which this correlation is used. Describe the blowdown heat transfer correlations used for the remainder of the break spectrum.

ANSWER

The justification for using the Hench-Levy CHF correlation to a system undergoing a rapid depressurization can be shown by examining the fuel rod time constant, the vessel depressurization rate, and the core inlet flow rate. Fundamentally, the CHFR is evaluated using a model which simulates the BWR 49 fuel rod bundle. The basic input consists of time varying pressure, core inlet flow, and core power which have been determined by other calculations. The model includes axial, radial, and local power distribution as well as distributed loss coefficients. The BWR fuel rod time constant is approximately 10 seconds. The maximum vessel depressurization rate would be approximately 50 to 100 psi/sec depending on the postulated break of either one recirculation line or one steamline at the vessel respectively. At rated core flow, it would take approximately 0.3 seconds for the coolant to travel through the core. Even under degraded flow conditions, the flow transit time in the core is not drastically altered primarily due to the voiding effect and its associated increase in velocity.

The average depressurization of the coolant per axial node (20 nodes/core) would be about 1 psi/sec. Furthermore, since the time constant of the fuel is approximately 10 seconds the node surface heat flux variation during the transit time of the coolant would be negligible. Therefore, for all practical purposes, the coolant is subjected to quasi-steady conditions because the changes in the key parameters are not rapid and the Hench-Levy steady state CHF data can be applied. Additional discussion is given in the answer to Question I.A.4.

Another basis for applying the CHF correlation is that all evidence to date indicates that the use of steady-state CHF data for predicting transient CHF conditions is conservative even during truly rapid transients.[1] Therefore, by applying steady-state multirod CHF data to this transient analysis, there is an inherent factor of conservatism. Further margin exists in this analysis, especially at the end of the transient because the actual improvement in CHF which occurs at pressures down to 600 psi over that at 1000 psi was neglected.

(1) Tong, L. S. "Transient CHF Prediction" Presented at ASME-AICHE Heat Transfer Conference, Philadelphia, Aug 1968.

A third basis for applying the CHF correlation is that the steady state data cover the entire range of flow rates and qualities which exist during the loss of coolant transient. Therefore, a firm basis for confidently predicting the CHF conditions throughout the transient exists.

The Hench-Levy correlation is used over the entire break range as discussed below.

Small Breaks

The small breaks are similar to a pump trip transient since AC power is assumed lost at the initiation of the accident. The rate of change of all key parameters is very slow and the depressurization does not affect the pump coastdown rate. The coastdown momentum of the pumping system provides more than adequate core flow to insure an MCHFR greater than unity and therefore very high nucleate boiling coefficients. Essentially all of the stored heat in the fuel would be removed within less than four fuel time constants (i.e., 30 seconds) of nucleate boiling. Therefore, after 30 seconds of nucleate boiling, the maximum core surface heat flux would be reduced to approximately 4% of the steady operating value. This is significantly lower than the pool boiling CHF under those conditions and thus a high heat transfer coefficient will exist. Note that the peak heat flux for this plant is 354,000 Btu/hr ft^2 during normal operation, and that within 15 seconds, the power will have decayed such that the peak heat flux is below 100,000 Btu/hr ft^2. Below this heat flux no flow is required to maintain nucleate boiling, since the pool CHF is greater than this value. It should also be noted that the average heat flux in the core at time zero is only 118,000 Btu/hr ft^2, below the pool boiling CHF virtually from the start (pool boiling CHF at 1000 psia is >129,000 Btu/hr^2). Therefore, for small breaks any time a fuel node is covered a high nucleate boiling heat transfer rate can be assumed. If it is uncovered the node is assumed to have a convection coefficient of zero.

Large Breaks

For large breaks, i.e. greater than about 0.5 ft^2, the flow coastdown is affected by the depressurization and must be calculated by the reactor transient flow model described in detail in Appendix C. The Hench-Levy correlation is used in the transient critical heat flux model (Appendix E) to determine when the MCHFR drops to unity. The flow rates through the core are those calculated by the transient flow model which includes the coastdown flow and any contribution from any flashing in the bottom plenum when it occurs. Because the peak power bundle will reach the CHF condition long before the other bundles in the core, it is the one analyzed to determine the transient MCHFR in the reactor core. When one spot on one of the hot fuel rods dries out (i.e., when MCHFR = 1) the entire core is assumed to be insulated until either the MCHFR exceeds unity again, or until the core is reflooded or core spray reaches rated flow.

Thus, there are also only two heat transfer correlations used for large break analyses during blowdown. When the MCHFR is greater than unity, based on the Hench-Levy CHF correlation, the Jens-Lottes heat transfer correlation is used to obtain the nucleate boiling heat transfer coefficient. The nucleate boiling heat transfer coefficient is of the order of 10,000 B/ft^2 F hr or higher. If the surface heat transfer coefficient is above few hundred B/ft^2 F hr, the peak clad temperatures are unaffected by higher valves of heat transfer coefficient. This is because the heat transfer from the fuel is then limited by conduction through the fuel pin itself rather than the surface heat transfer coefficient.

When the MCHFR is less than unity the surface heat transfer coefficient is assumed to be zero. This is conservative because film boiling heat transfer coefficients would exist which are of the order of 100 to 1000 B/ft^2 F and would actually provide additional cooling during the blowdown phase.

QUESTION

I.A.6. We understand that the new "level swell" model has been used successfully to predict some data from the Humboldt Bay and Bodega Bay blowdown tests. Please indicate the results of the comparisons between analysis and experiment in sufficient detail to support use of the level swell model.

ANSWER

Mixture level and local properties in a vessel during loss of coolant determine core heat transfer environment and nature of blowdown. Mixture level predictions currently are being made with an analytical model[1]* which has been compared with experiments, and reasonable level swell comparisons have been made with EVESR steam blowdown tests [2] and CSE blowdown data [3].

It consistently has been stated and shown that calculated blowdown rates used in loss of coolant analyses are faster-than-expected [4]. Therefore an acceptable evaluation of the mixture level model should be uncoupled from the blowdown model. Ideal data to use in an evaluation of the mixture level model is a time-dependent plot of (1) actual level, (2) mass remaining in the vessel, and (3) vessel pressure. Data usually published do not include all three measurements. However, pressure-time traces for bottom blowdowns exhibit a "knee", characteristic of a sudden change from liquid (or mixture) to vapor blowdown. It is, therefore, reasonable to use the mixture level model with a blowdown which closely predicts the given pressure trace. Time at which the measured "knee" appears can be compared with the time required for mixture level to reach zero elevation.

It is the purpose of this work to compare predicted mixture level with selected measurements showing either a pressure-time "knee", or actual level measurement.

Flowing Quality and Bottom Blowdown

Blowdown rate depends on break geometry, vessel stagnation pressure, and stagnation enthalpy [4]. The actual value of stagnation enthalpy is determined partly by mixture properties in the vessel, and partly by the fact that vapor bubbles rise through liquid. The following figure indicates blowdown from a bottom location.

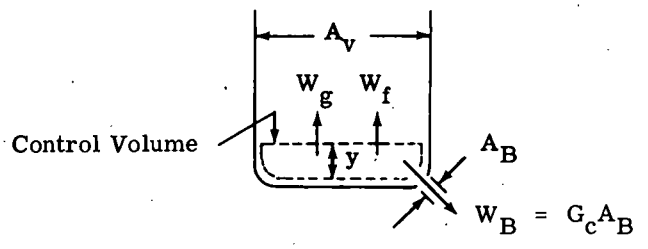

* References listed in back.

Total blowdown rate W_B is composed of vapor and liquid flows W_{gB} and W_{fB} :

$$W_{gB} = X_F W_B = X_F G_c A_B \quad (1)$$

$$W_{fB} = (1 - X_f) W_B = (1 - X_f) G_c A_B \quad (2)$$

The term X_F is flowing quality, or vapor mass flow fraction leaving the break. Critical flow rate per unit break area $G_c (P_o, h_o)$ can be considered a function of X_f and P_o if stagnation enthalpy h_o is expressed by

$$h_o = h_f (P_o) + X_F h_{fg} (P_o) \quad (3)$$

Vapor and liquid mass conservation equations are written as follows for the dotted control volume where elevation y is very small:

$$W_{gB} + W_g = o \quad (4)$$

$$W_{fB} + W_f = o \quad (5)$$

The terms W_g and W_f are upward flows of vapor and liquid at elevation y, expressed by [1]:

$$W_g = \frac{A_v V X}{v} \quad (6)$$

$$W_f = A_v u \left\{ \frac{V}{v} (1 - X) - \frac{u}{v_f} \right\} \quad (7)$$

Where V is bubble rise velocity relative to the vessel, u is bubble rise velocity in stationary liquid, and v is local mixture specific volume based on X, which is local instantaneous vapor mass fraction. Equation (1) through (7) can be combined to give:

$$\frac{A_B}{A_v u} = \frac{1}{G_c v_f} \frac{X}{X - X_F} = f (P_o, X, X_F) \quad (8)$$

Equation (8) relates P_o, X, and X_F to the property $\frac{A_B}{A_v u}$. If flowing quality X_F is zero, then stagnation enthalpy is $h_f (P_o)$, and bottom blowdown of saturated liquid occurs; i.e., the condition for $\frac{A_B}{A_v u}$ to be satisfied for bottom liquid blowdown is that

$$\left. \frac{A_B}{A_v u} \right|_{LIQ} \leq \frac{1}{G_c \left(P_o, h_f (P_o)\right) \cdot v_f (P_o)} \quad (9)$$

However, if the above inequality is not satisfied, vapor bubbles will be entrained in the blowdown flow, and Equation (8) must be used to determine X_F. Bottom liquid or mixture blowdowns from 1000 psig characteristically produce X in the range $0 \leq x \leq 0.10$. The corresponding effect on blowdown rate is small. It follows from Equation (8) therefore that

$$\frac{X_F}{X} \approx 1 - \frac{1}{G_c v_f \frac{A_B}{A_v u}} \tag{10}$$

Equation (10) can be used to help select test data for comparisons which can be closely approximated by liquid blowdown until the mixture level reaches the break.

Blowdown Rates and Pressure Traces

Calculated graphs already are available for liquid blowdown from 1000, 1250, and 2000 psia initial stagnation pressures [5] [6]. The graphs include a variable time scale with break area A_B as a parameter. Proper selection of an equivalent A_B * to bring theoretical and measured blowdown pressure traces into agreement will enable a better evaluation of the mixture level model.

Mixture Level Prediction

Mixture level has been calculated for vessel bottom blowdown from 1000 psia initial pressure with initial liquid level equal to 75 percent of the vessel overall height.

Where necessary, mixture level calculations can be made from the following equations [1] whenever $X_F > o$ from Equation (10):

$$\frac{Y_L(t^*)}{H} = \frac{A_v u}{A_B} \frac{v_g(t^*)}{v(o)} I_1(t^*) + \frac{Y_{Lo}}{H} \frac{M_f(t^*)}{M_{fo}} \left[\frac{v_g(t^*) S_{fg}(t^*)}{S_y(t^*) - S_{f(o)}} - v_{fg}(t^*) \right] \frac{1}{v_{fo}} \tag{11}$$

$$I_1(t^*) = -\int_o^{t^*} \frac{S_{f(o)} - S_f(t^*)}{S_g(t^*) - S_{f(o)}} dt^* \tag{12}$$

The time t* is given by

$$t^* = \frac{A_B}{M_o} t \tag{13}$$

Selected Tests for Comparison

Three tests were selected for this comparison from Bodega [7], Humboldt [8], and CSE [3] blowdowns. Pertinent experimental quantities are listed in Table I.A.1.

TABLE I.A.1

IMPORTANT EXPERIMENTAL QUANTITIES

	Bodega 30	Humboldt 17	CSE, B-15
Vessel Volume, ft^3	80	55	150
Initial Pressure, psia	1250	1250	$\approx$ 2000
Vessel Height H, ft	20	31.4	15
Vessel Area Av, ft^2	3.97	1.75	9.36
Break Area A_B, ft^2	.0573	.044	.0643
Initial Fluid Mass, lbs	2420	1795	6700
Initial Level Fraction $\frac{Y_{Lo}}{H}$	.685	.735	1.0
Equivalent Break Area A_B^*	.053	.0388	.0446
Value for $\frac{A_B^*}{A_v}$, $\frac{sec}{ft}$	.0134	.0222	.00477
The term $\frac{1}{G_o U_f}$, $\frac{sec}{ft}$	.00513	.00513	.00366

Bodega and Humboldt vessels were cylindrical without internal mechanical components to obstruct internal flows. The CSE vessel contained a dummy core plate.

The equivalent break areas were determined so that theoretical and measured pressure-time curves were closely aligned up to the pressure trace "knee". The quantity $\frac{A_B^*}{A_v u}$ was based on $u = 1.0$ foot per second bubble rise velocity, which seems to be more characteristic of small vessels. All three cases show that $\frac{A_B^*}{A_v u}$ is larger than the term $\frac{1}{G_{fc} U_f}$ initially so that mixture blowdown is assured. (G_{fc} decreases as pressure drops so that mixture blowdown is assured throughout the blowdown.) It follows that Equation (11) and (12) can be applied for necessary calculations.

Rather than calculate level curves for Bodega 30 and Humboldt 17, it was decided to make an approximate comparison with already available calculations from initial vessel pressures of 1000 psia. The tests begin at 1250 psia. Figures I.A.7 and I.A.8 show true vessel pressure traces with attention called to the "knee". The lower half of each graph gives mixture level calculations based on 1000 psia, and 75 percent initial water level. A dotted curve also is shown, based on the appropriate $\frac{A_B^*}{A_v u}$. When mixture level reaches zero, the pressure "knee" should occur. Even though the calculation is based on 1000 psia and the tests were run from 1250 psia, mixture level disappearance was predicted within 12.5 per cent using the model described and this is a direct index of its accuracy..

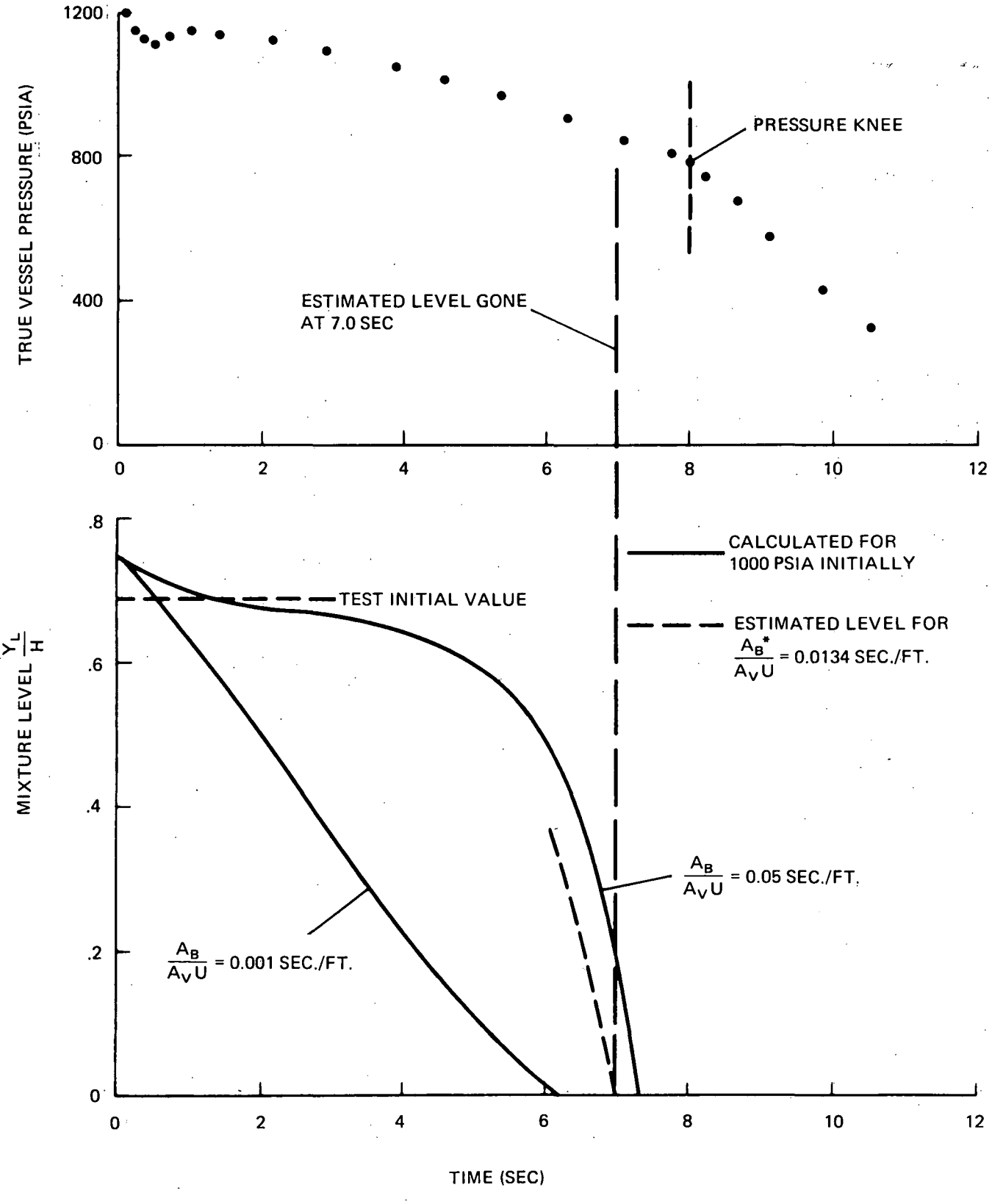

Fig I.A.7 Vessel Pressure And Level Traces – Bodega 30

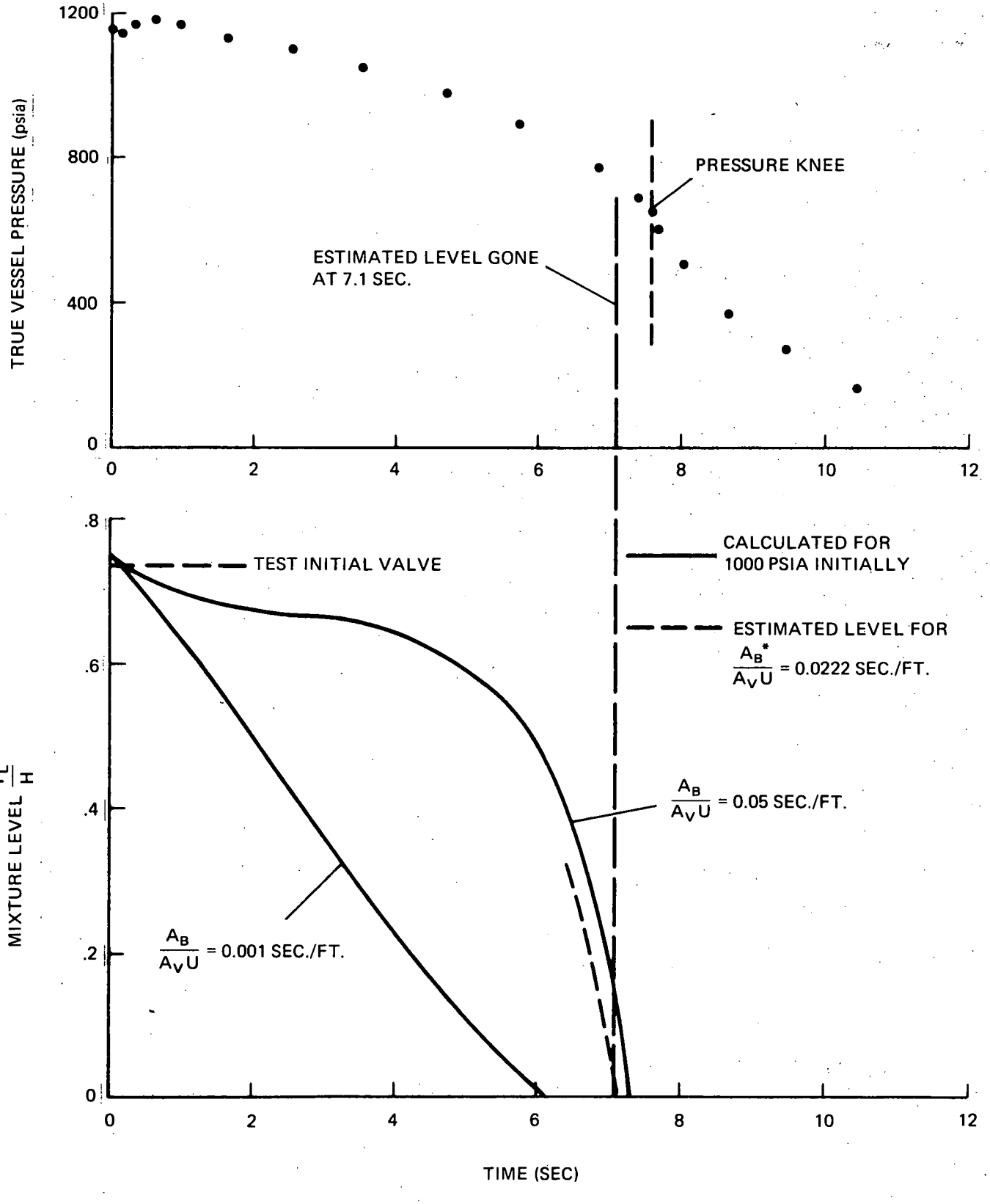

Fig. I.A.8 Vessel Pressure And Level Traces – Humboldt 17

The CSE Data [3] in Fig. I.A.9 includes both pressure, mass remaining, and level, for comparison with the mixture level model. Comparing only the level data in Figure I.A.9 it is seen that a bubble rise velocity between 0.5 fps and 1.0 fps brackets the CSE measured level. Note that the level swell model is not applied to the test data until the system is saturated. Note also that the 0.5 fps curve shows liquid vanishing at about the right time as indicated by the knee in the experimental curve. Thus reasonable agreement is also shown with the CSE data.

Additional comparison with the only other available data is discussed in Reference 1 in which the level rise data from EVESR given in Reference 2 is discussed. Efforts on the level rise phenomena are continuing with respect to model improvement. Additional effort is also continuing toward comparison with any additional data as it becomes available.

It is concluded from the comparisons with currently available data that the model has sufficient accuracy for predicting level rise.

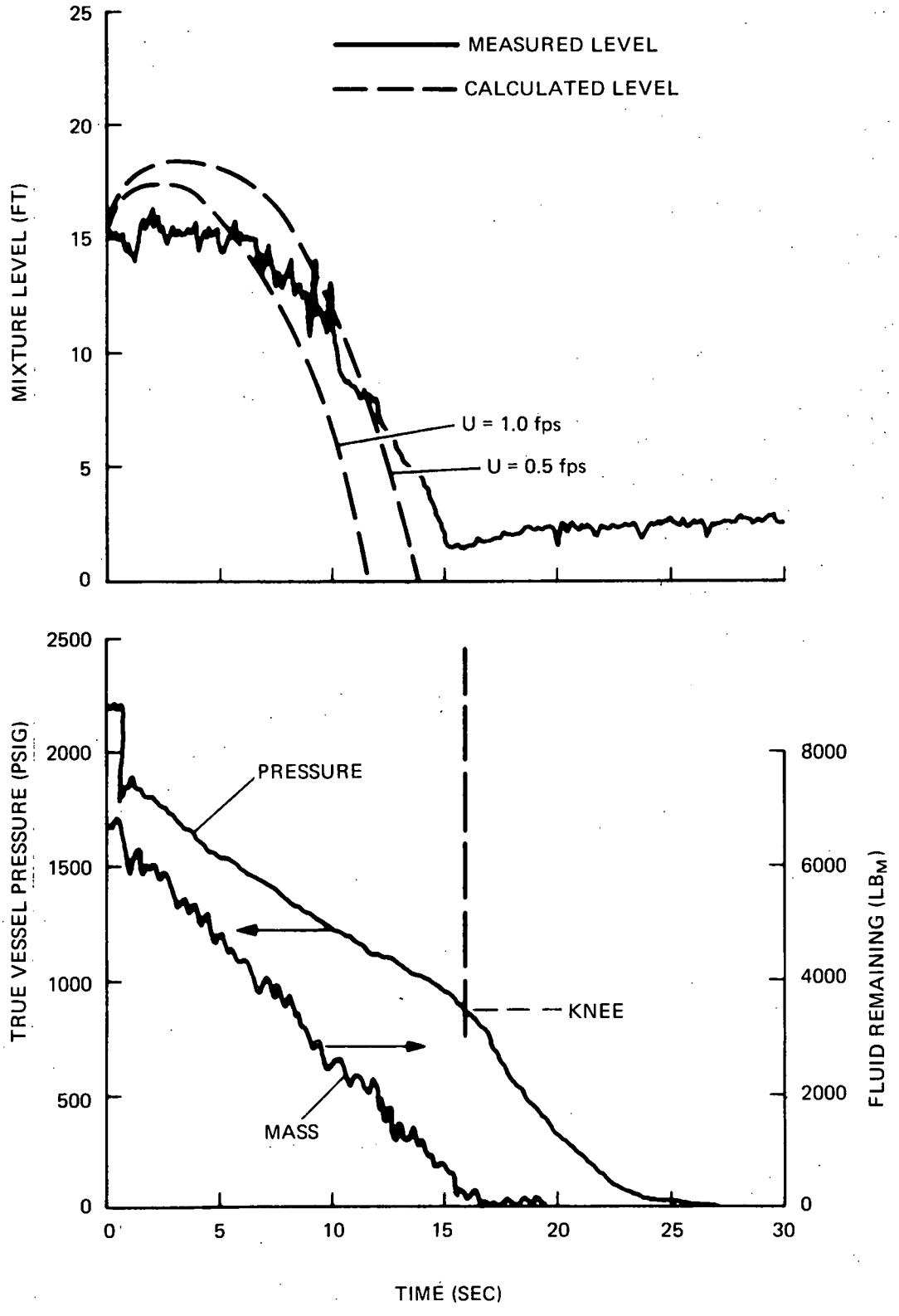

Fig I.A.9 Vessel Pressure And Level Traces – CSE Data, Run B-15

Notation

Major Symbols

A	Area
G	Mass flow rate per unit area
H	Vessel height
h	Specific enthalpy
M	Mass
P	Pressure
s	Specific entropy
t	Time
U	Rubble rise velocity relative to liquid
v	Specific volume
W	Flow rate
X	Homogeneous quality
X_F	Flowing quality
Y_L	Mixture level

Subscripts

B	Break
C	Critical flow
f	Saturated liquid
fg	Vaporization
g	Saturated vapor
o	Stagnation, or initial value

References

1. Moody, F. J., "Liquid-Vapor Action in a Vessel During Blowdown," APED-5177, 1966.

2. Ianni, F. W.: Fritz, J. R.; and Law, D. D., "Design and Operating Experiences of the ESADA Vallecitos Experimental Superheat Reactor (EVESR)," APED-4784, 1965.

3. "Nuclear Safety Quarterly Report, Feb., March, April, 1968, for Nuclear Safety Branch of USAEC Division of Reactor Development and Technology," BNWL-885, October, 1968.

4. Moody, F. J., "Maximum Two-Phase Vessel Blowdown from Pipes," APED-4827, 1965.

5. Moody, F. J., "Perfect Nozzle Blowdown Study," APED-4398, 1963.

6. Moody, F. J., "An Analytical Model for Pressure Suppression," APED-4734, 1964.

7. "Preliminary Hazards Summary Report, Bodega Bay Atomic Park Unit No. 1," PG&E, Dec. 28, 1962.

8. Robbins, C. H., "Tests of a Full Scale 1/48 Segment of the Humboldt Bay Pressure Suppression Containment," GEAP-3596, 1960.

QUESTION

I. B In Amendment No. 7 for Unit 2 and Amendment No. 8 for Unit 3, the number of safety valves was reduced from twenty to eight, with individual valve capacity remaining constant. Please provide sufficient summary technical information required by code in accordance with ASME Section III, N910.2 and a discussion of the margin between the peak allowable pressure and the peak vessel pressure for the transient postulated in Section 4.4.2 but assuming only a high pressure scram. For both the pressure scram and the flux scram transients, show that the assumptions used in the calculations are conservative with respect to the proposed technical specifications for safety system settings (Sections 2.2 and 2.3), control rod insertion times (Section 3.3.A.3), and the number of rods valved out of service (Section 3.3.A.5).

ANSWER

Introduction

Prior to 1967, the design capacities of the spring safety valves of APED's nuclear reactors were determined according to the requirements of Section I, Power Boilers, of the ASME Boiler and Pressure Vessel Code, P269-P290. Under the provision of this code, no credit was allowed for reactor scram as a complementary pressure protection device. Thus the required safety valve capacities were sized assuming essentially instantaneous isolation of the pressure vessel with no pressure relief other than that from the safety valves.

With the inclusion of Section III, Nuclear Vessels, to the ASME Boiler and Pressure Vessel Code, credit is taken for the scram protection system as a pressure protection device when determining the required safety valve capacities of nuclear vessels. The General Requirements for Protection against overpressure as given in Article 9 of Section III of the code allows this design practice. In addition, AEC and Industry Standards organizations have already prepared tentative reactor vessel overpressure protection criteria compatible with the ASME Code provision, which allows credit for an indirect scram of the reactor protection system. In order to clarify the differences, both the old and new design bases for sizing the safety valves are presented below.

A. Old Design Basis. The primary system safety valves shall be sized to limit the primary system pressure, including transients, to the limits expressed in Section I of the ASME Boiler and Pressure Vessel Code. No credit will be taken for reactor scrams, or for power operated relief valves, sprays, or for other power operated pressure relief devices. Sizing will be on this basis when applied to a full turbine trip with bypass system failure.

Note that there are two points related to probability in the above basis. First, with no scram credit, the probability of failure of the scram protection system is unrealistically assumed to be unity. Second, the reliability of safety valve system components is assumed to be unity and the code thereby permits meeting code limits without margin.

B. New Design Basis. The primary system safety valves shall be sized to limit the primary system pressure, including transients, to the limits expressed in Section III of the ASME Boiler and Pressure Vessel Code. No credit will be taken for a turbine trip scram, or for power operated pressure relieving devices. Credit will be taken for subsequent protection system action, such as neutron flux scram or reactor high pressure scram. Sizing will be on this basis when applied to a full turbine trip with bypass system failure, starting from turbine design conditions of operation.

Note here, the more realistic approach in taking credit for an indirect scram as allowed by the ASME Code and recommended by the AEC criteria. The probability of failure of the available trip scram however is still assumed to be unity and the basis still permits sizing to a capacity requirement which just prevents vessel overpressure.

The above described bases are used to determine the minimum safety valve capacities which conform to the ASME code limits. Current G. E. engineering design practice results in a number of safety valves which exceeds the minimum code requirement, thus providing additional design margin.

Over-Pressure Protection Analyses

Applying both of the above described design bases, transient analyses were made specifically for the Dresden 2, 3 nuclear power plants. The results of these analyses are shown on Figure I. B. 1.

The purpose of the analyses was to determine the minimum safety valve capacity requirements which would conform to the applicable code and design basis. Also to be determined were the pressure margins resulting from additional capacity.

The old code and design basis disallows any scram credit, thus requiring all safety valve protection. It was determined that, for this case, the minimum capacity of safety valves to satisfy all requirements is 150 percent of turbine design steam flow. With spring valves of approximately 0.63 million pounds per hour the minimum requirement is thus 23 safety valves.

The new code and design basis permits credit for the flux scram in vessel pressure protection. For the Dresden 2, 3 plants, the minimum capacity for conformance to all requirements under the conditions stated is approximately 20 percent of turbine design steam flow. Thus for this case the minimum requirement would be 3 valves.

Analyses for the trip scram and pressure scram situations were also made and it was determined that one valve would satisfy all requirements if trip scram were allowed and that 5 valves would be the minimum required if only the backup pressure scram were allowed.

Figure I. B. 1 shows the expected pressure peaks for the Dresden 2, 3 plants that would result as a function of the number of safety valves for the turbine trip without bypass transient. The curves of peak pressure versus capacity are plotted for the cases of no scram, pressure scram, flux scram and trip scram.

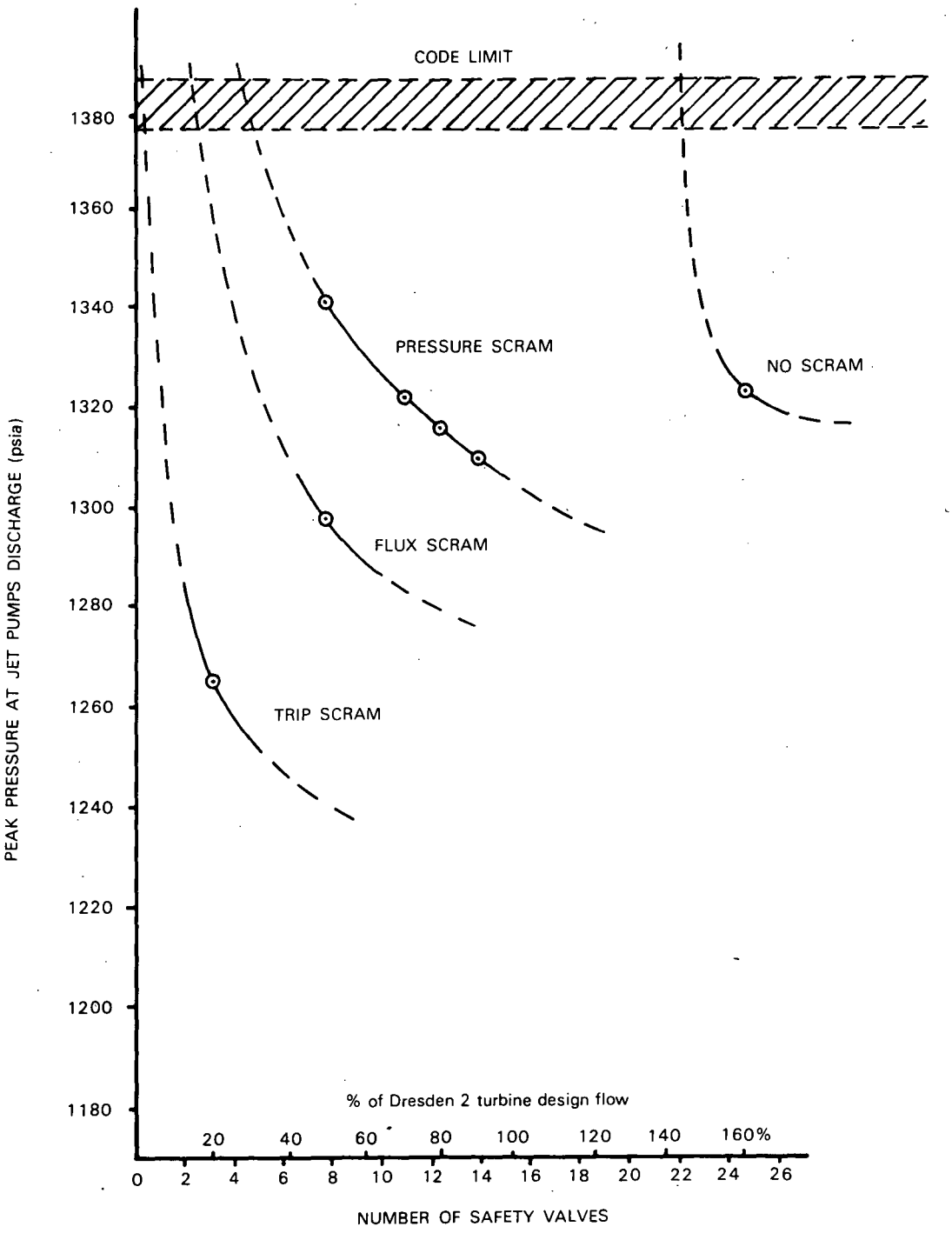

FIGURE I.B.1 DRESDEN 2, 3 PRESSURE PEAKS VS. CAPACITY TURBINE TRIP WITHOUT BYPASS TRANSIENT

Reliability of Pressure Protection

Using the above determined minimum capacities, a reliability analysis was conducted for the Dresden 2, 3 plants. The latest available reliability data for the operation of safety valves and for operation of the scram protection system were used in the analysis. Figure I. B. 2 shows some of the results of this analysis. Plotted on the figure are curves showing the probability of exceeding the ASME pressure vessel code limits against the number of safety valves installed. The curves are the mean values between the best and worst reliability data for the different scram or no scram conditions, where 10^{-6} means exceeding code once in a million incidents.

Table I. B. 1 summarizes the important probability values from the figure.

TABLE I. B. 1

PROTECTION DEVICES ALLOWED	PROBABILITY OF EXCEEDING CODE LIMITS					
	Number of Valves					
	1	3	5	8	23	25
Safety valves + all scrams	$8x10^{-3}$	$9x10^{-6}$	$3x10^{-8}$	$1x10^{-8}$	$4x10^{-9}$	$4x10^{-9}$
Safety valves + flux & pressure scram	1.0	$(2.5x10^{-2})$	$8x10^{-6}$	$3x10^{-8}$	$1x10^{-8}$	$1x10^{-8}$
Safety valves + pressure scram	1.0	1.0	$4x10^{-2}$	$1x10^{-6}$	$3x10^{-8}$	$3x10^{-8}$
Safety valves only, no scram	1.0	1.0	1.0	1.0	$(3x10^{-1})$	$1x10^{-3}$

The circled values in the table show the probabilities of exceeding code limits with the minimum number of valves which conform to these limits for the flux scram and no scram cases described earlier.

Notice that for the cases where flux scram is allowed, there is no discernable improvement in actual reliability in going from 8 safety valves to 25 safety valves. Also note the differences in reliability between cases where different scram options are allowed. These differences are small when compared to the absolute reliability obtained when any scram is allowed.

The 10^{-5} threshhold value of probability of exceeding code limits as shown on Figure I. B. 2 is a recommended maximum value when allowing credit for the scram protection system in preventing vessel overpressure. This threshhold is shown in Table I. B. 1 as the "staircase" bisecting the table. The 10^{-5} value is an IEEE recommended scram reliability figure applied to the nuclear industry.

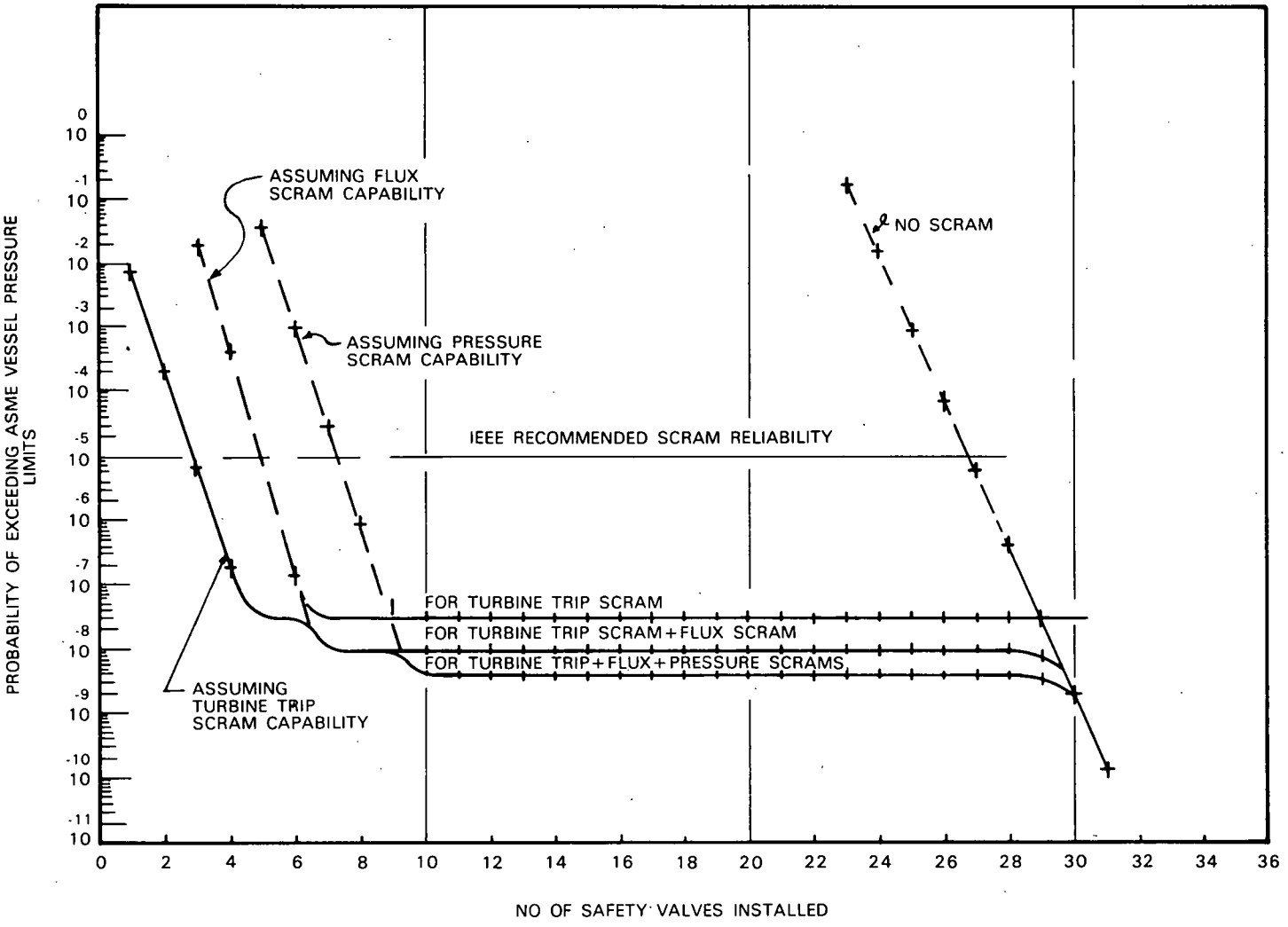

FIGURE I.B.2 DRESDEN 2, 3 VESSEL PRESSURE PROTECTION (TWO YEAR VALVE TEST SCHEDULE)

4/1/96

Dresden 2, 3 Safety Valve Design Analyses

Transient Analyses were made for the Dresden 2, 3 plants to size the required capacities of the safety valves by applying both the old and new design bases. Also considered in these design analyses were the the results of the reliability studies and the application of reasonable pressure margin requirements. A description of the results of these analyses follows.

A. Safety Valve Sizing Under Old Design Basis. Allowing no credit for any reactor scram and no credit for bypass action or other pressure relieving device, the transient analyzed was a turbine trip with failure of bypass and all pressure relief systems except the safety valves themselves. The reactor power level at the start of the transient was 2527 MWt, or that power necessary to achieve turbine design steam flow.

Following this reactor isolation, the vessel pressure increases until limited by the opening of the safety valves. The peak pressure allowable is 1375 psig or 110 percent of the 1250 psig vessel design pressure according to the Section I ASME Boiler and Pressure Vessel Code. The safety valves were spread in 10 psi intervals between 1210 psig and 1250 psig, satisfying code specifications that at least one valve must be set at or below the vessel design pressure and that the set point of the last valve be no higher than 105 percent of design pressure. Although, as shown previously, only 23 valves are required to meet minimum code requirements, the plant was sized for 25 safety valves providing relief in excess of 160 percent of turbine design steam flow. The additional valves provide adequate pressure margin as required by engineering practice and increases the reliability of the safety valve system in preventing pressure increase in excess of code limits.

With 25 valves, the pressure at the bottom of the vessel is about 1240 psig when the first safety valves lift and about 1280 psig when the last valves lift. Both values are clearly within code limits. Vessel dome pressure peaks at about 1280 psig at 3.3 seconds with the pressure peak at the bottom of the vessel near 1310 psig. Thus, with 25 safety valves, adequate margin is provided between the transient pressure peak at the 1375 psig code limit.

B. Safety Valve Sizing Under New Design Basis. The transient analyzed was the same as that described in the previous analysis except that, for this case, credit was allowed for neutron flux scram. The neutron flux scram of the protection system complements the action of the safety valves in accomplishing overpressure protection.

Under the Section III ASME Boiler and Pressure Vessel code the peak allowable pressure is also 110 percent of vessel design pressure or 1375 psig. The set points of the safety valves were again spread in 10 psi intervals between 1210 and 1240 psig to satisfy the code specifications on the lowest and highest set points. As shown previously only 3 valves would be required to just meet code requirements. For this sizing transient, however, 8 safety valves were used. These 8 valves provide relief in excess of 50 percent of turbine design steam flow. The additional valves provide adequate pressure margin and increase the reliability of the safety valve system. The G. E. engineering design for Dresden 2, 3 is well within the code pressure protection requirements when only the slower pressure scram rather than neutron flux scram is operative, thus adding conservatism to the design. In addition, the

resulting 8 safety valves assure that the probability that the safety valve system with scram credit will exceed the code limits is less than the recommended value of 10^{-5}.

After the fast isolation resulting from the stop valve closure with no initial relief, the reactor pressure increases until limited by the combined action of the flux scram and the opening of the safety valves. With 8 valves and flux scram, the pressure at the bottom of the vessel is about 1240 psig when the first valves open and about 1270 psig when the last valves open thus conforming to Code limits. Vessel dome pressure peaks at about 1260 psig at 3.5 seconds with the peak at the bottom of the vessel near 1290 psig. Thus the 8 valve with flux scram system provides adequate margin below the 1375 psig Code imit.

A comparison of the two pressure transients described above is shown in Figure I. B. 3. Notice that the pressure rise rate for the case with scram is already decreasing, as a result of the scram, before the set point of the first safety valve is reached.

The curve showing the pressure scram only transient has not been shown because the Code requires that only the flux scram requirement need be met. It can be seen from Figure I.B.1, however, that the Code safety limit will not be exceeded even considering the pressure scram only.

The transient calculations were made assuming the values listed in the Technical Specifications for safety system settings, control rod insertion times, and the minimum shutdown margin (Section 3.3.A.5). The number of rods which are specified inoperable, whether they are in or out of the core, was considered insofar as the minimum shutdown margin is met. The minimum pressure difference between curve B and the Code specified limit on Figure I.B.3 represents the margin available when the Technical Specification values are used.

Conclusion

In view of the extremely high reliability of the scram protection system, the new design basis of sizing safety valves with indirect scram credit is highly realistic. Scram credit is allowed under Section III of the ASME Boiler and Pressure Vessel Code and defined by tentatively established overpressure protection criteria. Design practices of sizing the safety valves under the new code can provide equivalent or in some cases even better pressure protection and system reliability within the new code's constraints and assumptions than is provided under the older code within its contraints and assumptions where no credit is allowed for the highly reliable scram systems.

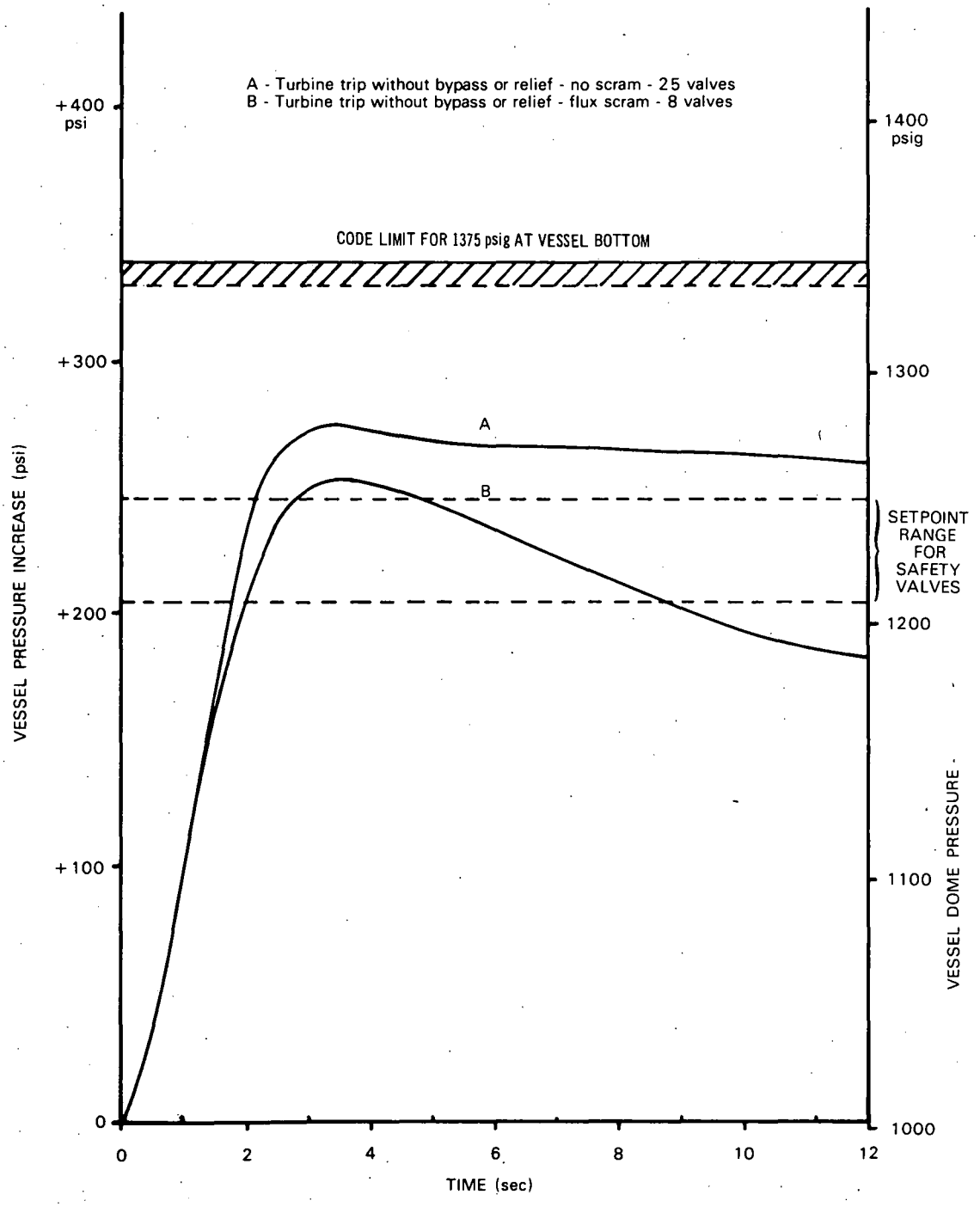

FIGURE I.B.3 DRESDEN 2, 3 SAFETY VALVE TRANSIENTS